

¹ The Evolution of Siphonophore Tentilla as Specialized Tools for Prey Capture

³ Alejandro Damian-Serrano^{1,‡}, Steven H.D. Haddock², Casey W. Dunn¹

⁴ ¹ Yale University, Department of Ecology and Evolutionary Biology, 165 Prospect St.,
⁵ New Haven, CT 06520, USA

⁶ ² Monterey Bay Aquarium Research Institute, 7700 Sandholdt Rd., Moss Landing, CA
⁷ 95039, USA

⁸ [‡] Corresponding author: Alejandro Damian-Serrano, email: alejandro.damianserrano@
⁹ yale.edu

¹⁰ Abstract

¹¹ Predators have evolved dedicated body parts to capture and subdue prey. As different
¹² predators specialize on distinct prey taxa, their tools for prey capture diverge into a variety
¹³ of adaptive forms. Studying the evolution of predation is facilitated by a predator clade
¹⁴ with structures used exclusively for prey capture and with significant morphological varia-
¹⁵ tion. Siphonophores, a clade of colonial cnidarians, satisfy these criteria particularly well,
¹⁶ capturing prey with their tentilla (tentacle side branches). Earlier work has shown that
¹⁷ extant siphonophore diets correlate with the different morphologies and sizes of their tentilla
¹⁸ and nematocysts. We hypothesize that evolutionary specialization on different prey types
¹⁹ has driven the phenotypic evolution of these characters. To test this hypothesis, we: (1)
²⁰ measured multiple morphological traits from fixed siphonophore specimens using microscopy
²¹ and high-speed video techniques, (2) built a phylogenetic tree of 45 species, and (3) analyzed
²² the evolutionary associations between siphonophore nematocyst characters and prey type
²³ data from the literature. Our results show that siphonophore tentillum structure has strong
²⁴ evolutionary associations with prey type and size specialization, and suggest that shifts
²⁵ between prey-type specializations are linked to shifts in tentillum and nematocyst size and

26 shape. In addition, we generated hypotheses about the diets of understudied siphonophore
27 species based on these characters. Thus, the evolutionary history of tentilla shows that
28 siphonophores are an example of ecological niche diversification via morphological innovation
29 and evolution. This study contributes to understanding how morphological evolution has
30 shaped present-day oceanic food webs.

31 **Keywords**

32 Siphonophores, tentilla, nematocysts, predation, specialization, character evolution

33

34 Most animal predators have characteristic biological tools that they use to capture and
35 subdue prey. Raptors have claws and beaks, snakes have fangs, wasps have stingers, and
36 cnidarians have nematocyst-laden tentacles. The functional morphology of these structures
37 tend to be finely attuned to their ability to successfully capture specific prey (Schmitz
38 2017). Long-term adaptive evolution in response to the defense mechanisms of the prey (*e.g.*
39 avoidance, escape, protective barriers) leads to modifications that can counter those defenses
40 The more specialized the diet of a predator is, the more specialized its tools need to be to
41 meet the specific challenges posed by the prey. Understanding the relationships between
42 predatory specializations and morphological specializations is necessary to contextualize the
43 phenotypic diversity of predators, and to quantify the importance of ecological diversification
44 in generating this diversity.

45 Siphonophores (Cnidaria : Hydrozoa) are a clade of organisms bearing modular structures
46 that are exclusively used for prey capture: the tentilla (Fig. 1). These present a significant
47 morphological variation across species (Mapstone 2014) (Fig. 2), which makes them an
48 ideal system to study the relationships between functional traits and prey specialization. A
49 siphonophore is a colony bearing many feeding polyps (Fig. 1), each with a single tentacle,
50 which branches into several tentilla carrying the functional cnidocytes (specialized neural cells

51 carrying nematocysts, the stinging capsules). Unlike most other cnidarians, siphonophores
52 carry their tentacle nematocysts in extremely complex and organized batteries (Skaer 1988)
53 built into their tentilla. While nematocyst batteries and clusters in other cnidarians are simple
54 static scaffolds for cnidocytes, siphonophore tentilla have their own reaction mechanism,
55 triggered upon encounter with prey. When it fires, a tentillum undergoes an extremely
56 fast conformational change that wraps it around the prey, maximizing the surface area
57 of contact for nematocysts to fire on the prey (Mackie et al. 1987). In addition, some
58 species have elaborate fluorescent and bioluminescent lures on their tentilla to attract prey
59 with aggressive mimicry (Purcell 1980; Haddock et al. 2005; Haddock and Dunn 2015).
60 Siphonophores bear four major nematocyst types in their tentacles and tentilla. The largest
61 type, heteronemes, have open-tip tubules characterized by bearing a distinctly wider spiny
62 shaft at the proximal end of the everted tubule. These are typically found flanking the
63 proximal end of the cnidoband. The most abundant type, haplonemes, have no distinct shaft,
64 but similarly to heteronemes, their tubules have open tips and can be found in the cnidoband.
65 Both heteronemes and haplonemes bear short spines along the tubule and can be toxic and
66 penetrate the surface of some prey types. In the terminal filament, siphonophores bear two
67 other types of nematocysts, characterized by their adhesive function, closed tip tubules, and
68 lack of spines on the tubule. These are the desmonemes (a type of adhesive coiled-tubule
69 spironeme), and rhopalonemes (a siphonophore-exclusive nematocyst type with wide tubules).

70 Many siphonophore species inhabit the deep pelagic ocean, which spans from ~200m to
71 the oceanic seafloor. This habitat has fairly homogeneous physical conditions and stable
72 zooplankton abundances and composition (Robison 2004). With a relatively predictable
73 prey availability, ecological theory would predict evolution to drive coexisting siphonophore
74 lineages towards specialization, increasing their feeding efficiencies and reducing interspecific
75 competition (Simpson 1944; Hardin 1960; Hutchinson 1961). If this prediction holds true,
76 we expect the prey capture apparatus morphologies of siphonophores to diversify with the
77 evolution of increased specialization on a variety of prey types in different siphonophore

78 lineages.

79 Specialization is often thought to be an evolutionary ‘dead end’, meaning that specialized
80 lineages are unlikely to evolve into generalists or to shift the resource for which they are
81 specialized (Futuyma and Moreno 1988). However, recent studies have found that interspecific
82 competition can favor the evolution of resource generalism (Stireman-III 2005; Johnson et
83 al. 2009) and resource switching (Hoberg and Brooks 2008). Here we examine three
84 alternative hypotheses on siphonophore trophic specialization: (1) predatory specialists
85 evolved from generalist ancestors; (2) predatory specialists evolved from ancestral predators
86 which specialized on a different resource, switching their primary prey type; and (3) predatory
87 generalists evolved from specialist ancestors.

88 The study of siphonophore tentilla and diets has been limited in the past due to the
89 inaccessibility of their oceanic habitat and the difficulties associated with the collection of
90 fragile siphonophores. Thus, the morphological diversity of tentilla has only been characterized
91 for a few taxa, and their evolutionary history remains largely unexplored. Contemporary
92 underwater sampling technology provides an unprecedented opportunity to explore the trophic
93 ecology (Choy et al. 2017) and functional morphology (Costello et al. 2015) of siphonophores.
94 In addition, well-supported phylogenies based on molecular data are now available for these
95 organisms (Munro et al. 2018). These advances allow for the examination of relationships
96 between modern siphonophore form, function, and ecology, as well as reconstructing their
97 evolutionary history.

98 The few pioneering studies that have addressed the relationships between tentilla and
99 diet suggest that siphonophores are a robust system for the study of predatory specialization
100 via morphological diversification. (Purcell 1984) and (Purcell and Mills 1988) showed clear
101 relationships between diet, tentillum, and nematocyst characters in co-occurring epipelagic
102 siphonophores. These correlations, while studied for a small subset of extant epipelagic
103 siphonophore species, might be generalizable to all siphonophores. We hypothesize that
104 these relationships reflect correlated evolution between prey selection and tentillum (and

¹⁰⁵ nematocyst) traits. Furthermore, we hypothesize that with an extensive characterization of
¹⁰⁶ tentilla morphology, we can generate hypotheses about the diets of understudied siphonophore
¹⁰⁷ species.

¹⁰⁸ In addition, our study design allows us to address other interesting questions about the
¹⁰⁹ morphology and evolution of these unique structures. In particular, we aim to address the
¹¹⁰ evolutionary origins of giant tentilla, the character integration of tentilla, the evolution of
¹¹¹ the extreme shapes of siphonophore nematocysts (Thomason 1988), and the mechanical
¹¹² implications of tentillum morphologies on cnidoband discharge.

¹¹³ In this study, we characterize the morphological diversity of tentilla and their nematocysts
¹¹⁴ across a broad variety of shallow and deep sea siphonophore species using modern imaging
¹¹⁵ technologies, we expand the phylogenetic tree of siphonophores by combining a broad taxon
¹¹⁶ sampling of ribosomal gene sequences with a transcriptome-based backbone tree, and we
¹¹⁷ explore the evolutionary histories and correlations among diet, tentillum, and nematocyst
¹¹⁸ characters.

¹¹⁹ Methods

¹²⁰ *Tentillum morphology* – The morphological work was carried out on siphonophore specimens
¹²¹ fixed in 4% formalin from the Yale Peabody Museum Invertebrate Zoology (YPM-IZ) collection
¹²² (accession numbers in Appendix 1). These specimens were collected intact across many years of
¹²³ fieldwork expeditions, using blue-water diving (Haddock and Heine 2005), remotely operated
¹²⁴ vehicles (ROVs), and human-operated submersibles. Tentacles were dissected from non-larval
¹²⁵ gastrozooids, sequentially dehydrated into 100% ethanol, cleared in methyl salicylate, and
¹²⁶ mounted onto slides with Canada Balsam or Permount mounting media. The slides were
¹²⁷ imaged as tiled z-stacks using differential interference contrast (DIC) on an automated stage
¹²⁸ at YPM-IZ (with the assistance of Daniel Drew and Eric Lazo-Wasem) and with laser point
¹²⁹ confocal microscopy using a 488 nm Argon laser that excited autofluorescence in the tissues.
¹³⁰ Thirty characters (defined in Appendix 2) were measured using Fiji (Collins 2007; Schindelin

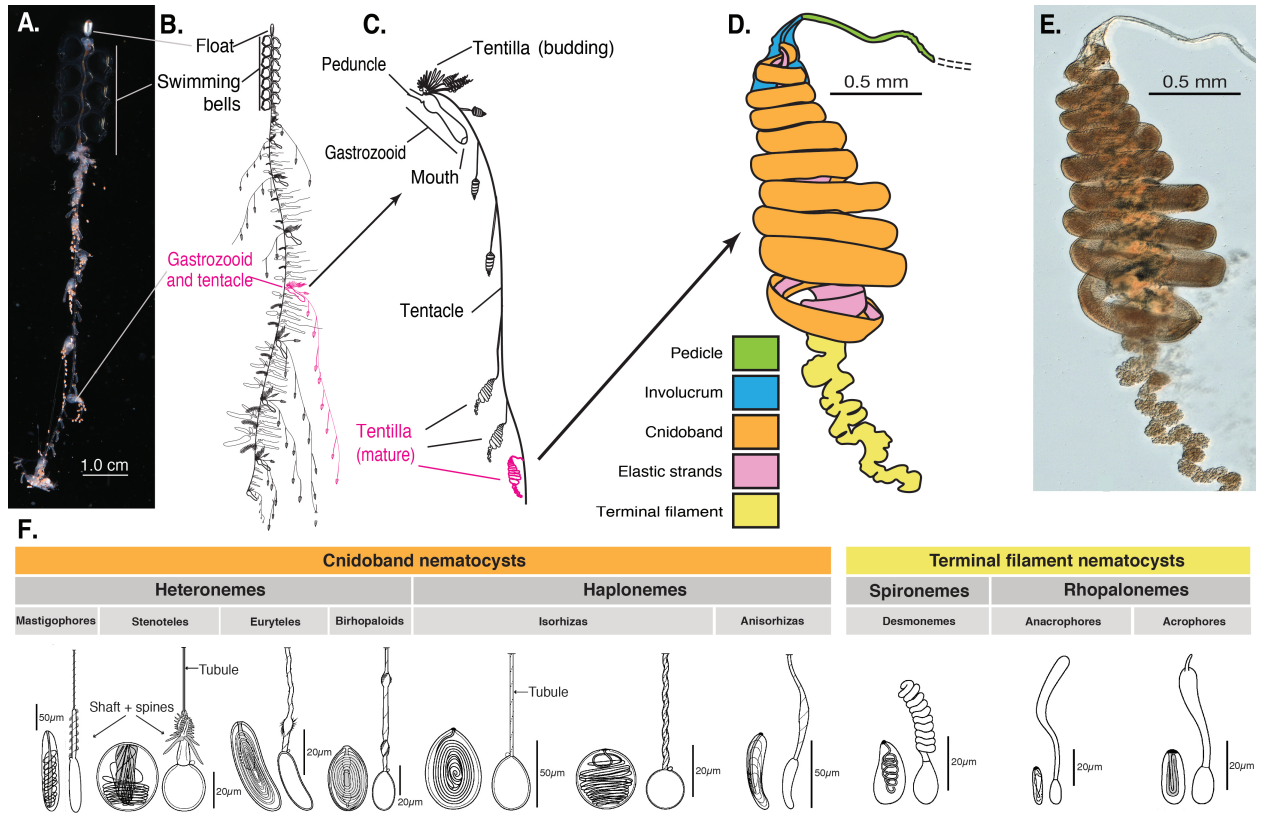


Figure 1: Siphonophore anatomy. A - *Nanomia* sp. siphonophore colony (photo by Catriona Munro). B,C - Illustration of a *Nanomia* colony, gastrozooid, and tentacle (by Freya Goetz). D - *Nanomia* sp. Tentillum illustration and main parts. E - Differential interference contrast micrograph of the tentillum illustrated in D. F - Nematocyst types (illustration reproduced with permission from Mapstone 2014), hypothesized homologies, and locations in the tentillum. Undischarged to the left, discharged to the right.

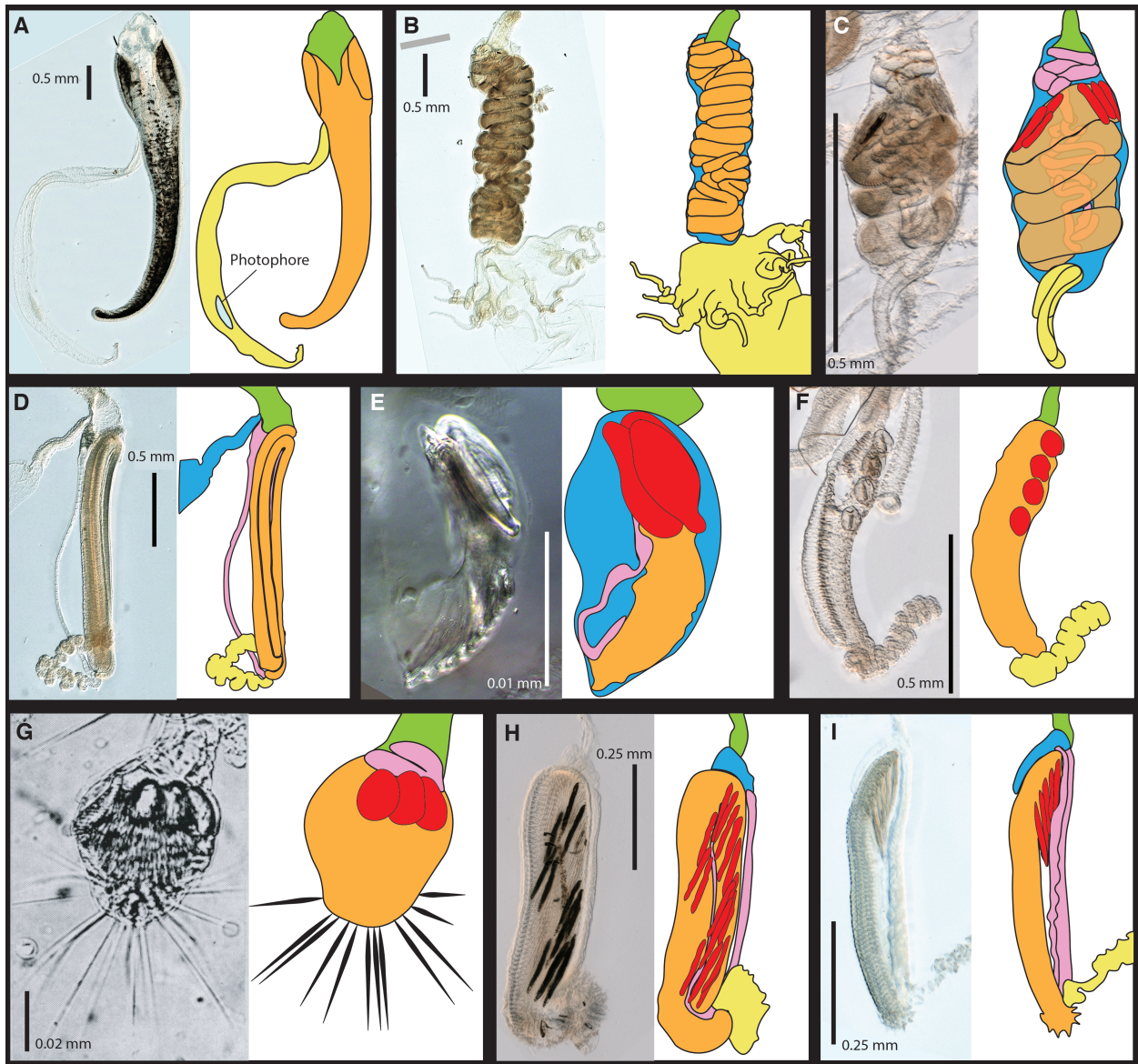


Figure 2: Tentillum diversity plate. The illustrations delineate the pedicle (green), involucrum (blue), cnidoband (orange), elastic strands (pink), terminal structures (yellow). Heteroneme nematocysts (stenoteles in C,E,F,G and mastigophores in H,I) are depicted in red for some species. A - *Erenna laciniata*, 10x. B - *Lychnagalma utricularia*, 10x. C - *Agalma elegans*, 10x. D - *Resomia ornicephala*, 10x. E - *Frillagalma vityazi*, 20x. F - *Bargmannia amoena*, 10x. G - *Cordagalma* sp., reproduced from Carré 1968. H - *Lilyopsis fluoracantha*, 20x. I - *Abylopsis tetragona*, 20x.

¹³¹ et al. 2012). We did not measure the lengths of contractile structures (terminal filaments,
¹³² pedicles, gastrozooids, and tentacles), since they are too variable to quantify. We measured
¹³³ at least one specimen for 96 different species (Appendix 3, Fig. 3). Of these, we selected 38
¹³⁴ focal species across clades based on specimen availability and phylogenetic representation.
¹³⁵ Three to five tentacle specimens from each one of these selected species were measured to
¹³⁶ capture intraspecific variation.

¹³⁷ In order to observe the discharge behavior of different tentilla, we recorded high speed
¹³⁸ footage (1000-3000 fps) of tentillum and nematocyst discharge by live siphonophore specimens
¹³⁹ (26 species) using a Phantom Miro 320S camera mounted on a stereoscopic microscope. We
¹⁴⁰ mechanically elicited tentillum and nematocyst discharge using a fine metallic pin. We used
¹⁴¹ the Phantom PCC software to analyze the footage. For the 10 species recorded, we measured
¹⁴² total cnidoband discharge time (ms), heteroneme filament length (μm), and discharge speeds
¹⁴³ (mm/s) for cnidoband, heteronemes, haplonemes, and heteroneme shafts when possible (data
¹⁴⁴ in Appendix 4).

¹⁴⁵ *Siphonophore phylogeny* – The phylogenetic analysis included 55 siphonophore species
¹⁴⁶ and 6 outgroup cnidarian species (*Clytia hemisphaerica*, *Hydra circumcincta*, *Ectopleura*
¹⁴⁷ *dumortieri*, *Porpita porpita*, *Velella velella*, *Staurocladia wellingtoni*). The gene sequences
¹⁴⁸ we used in this study are available online (accession numbers in Appendix 5). Some of
¹⁴⁹ the sequences we used were accessioned in (Dunn et al. 2005), and others we extracted
¹⁵⁰ from the transcriptomes in (Munro et al. 2018). Two new 16S sequences for *Frillagalma*
¹⁵¹ *vityazi* (MK958598) and *Thermopalria* sp. (MK958599) sequenced by Lynne Christianson
¹⁵² were included and accessioned to NCBI. We aligned these sequences using MAFFT (Katoh
¹⁵³ et al. 2002) (alignments available in Dryad). We inferred a Maximum Likelihood (ML)
¹⁵⁴ phylogeny (Appendix 6) from 16S and 18S ribosomal rRNA genes using IQTree (Nguyen et
¹⁵⁵ al. 2014) with 1000 bootstrap replicates (iqtree -s alignment.fa -nt AUTO -bb 1000). We
¹⁵⁶ used ModelFinder (Kalyaanamoorthy et al. 2017) implemented in IQTree v1.5.5. to assess
¹⁵⁷ relative model fit. ModelFinder selected GTR+R4 for having the lowest Bayesian Information

158 Criterion score. Additionally, we inferred a Bayesian tree with each gene as an independent
159 partition in RevBayes (Höhna et al. 2016) (Appendix 7 and 9), which was topologically
160 congruent with the unconstrained ML tree. The *alpha* priors were selected to minimize prior
161 load in site variation.

162 Given the broader sequence sampling of the transcriptome phylogeny, we ran constrained
163 inferences (using both ML and Bayesian timetree approaches, which produced fully congruent
164 topologies (Appendix 6 and 7)) after fixing the 5 nodes that were incongruent with the
165 topology of the consensus tree in (Munro et al. 2018). This topology was then used to
166 inform a Bayesian relaxed molecular clock time-tree in RevBayes, using a birth-death process
167 (sampling probability calculated from the known number of described siphonophore species)
168 to generate ultrametric branch lengths (Appendix 8). Scripts available in Appendix 9.

169 *Feeding ecology* – We extracted categorical diet data for different siphonophore species
170 from published sources, including seminal papers (Biggs 1977; Purcell 1981, 1984; Andersen
171 1981; Mackie et al. 1987; Pugh and Youngbluth 1988; Bardi and Marques 2007), and
172 ROV observation data (Hissmann 2005; Choy et al. 2017) with the assistance of Elizabeth
173 Hetherington and C. Anela Choy (Appendix 10). We removed the gelatinous prey observations
174 for *Praya dubia* eating a ctenophore and a hydromedusa, and for *Nanomia* sp. eating *Aegina*,
175 since we believe these are rare events that have a much larger probability of being detected by
176 ROV methods than their usual prey, and it is not clear whether the medusae were attempting to
177 prey upon the siphonophores. Personal observations on feeding (from SHDH, CAC, and Philip
178 Pugh) were also included for *Resomia ornicephala*, *Lychnagalma utricularia*, *Bargmannia*
179 *amoena*, *Erenna richardi*, *Erenna laciniata*, *Erenna sirena*, and *Apolemia rubriversa*. In order
180 to detect coarse-level patterns in the feeding habits, the data were merged into feeding guilds.
181 The feeding guilds described here are: small-crustacean specialist (feeding mainly on copepods
182 and ostracods), large crustacean specialist (feeding on large decapods, mysids, or krill), fish
183 specialist (feeding mainly on actinopterygian larvae, juveniles, or adults), gelatinous specialist
184 (feeding mainly on other siphonophores, medusae, ctenophores, salps, and/or doliolids), and

generalist (feeding on a combination of the aforementioned taxa, without favoring any one prey group). These were selected to minimize the number of categories while keeping the most different types of prey separate. We extracted copepod prey length data from (Purcell 1984). To calculate specific prey selectivities, we extracted quantitative diet and zooplankton composition data from (Purcell 1981), matched each diet assessment to each prey field quantification by site, calculated Ivlev's electivity indices (Jacobs 1974), and averaged those by species (Appendix 11).

Statistical analyses – For subsequent comparative analyses, we removed species present in the tree but not represented in the morphology data, and *vice versa*. Although we measured specimens labeled as *Nanomia bijuga* and *Nanomia cara*, we are not confident in some of the species-level identifications, and some specimens were missing diagnostic zooids. Thus, we decided to collapse these into a single taxonomic concept (*Nanomia* sp.). All *Nanomia* sp. observations were matched to the phylogenetic position of *Nanomia bijuga* in the tree. We carried out all phylogenetic comparative statistical analyses in the programming environment R (Team 2017), using the Bayesian ultrametric species tree (Fig. 4), and incorporating intraspecific variation estimated from the specimen data as standard error whenever the analysis tool allowed it (Appendix 3). R scripts available in Dryad. For each character (or character pair) analyzed, we removed species with missing data and reported the number of taxa included. We tested each character for normality using the Shapiro-Wilk test (Shapiro and Wilk 1965), and log-transformed those that were non-normal.

We fitted different models generating the observed data distribution given the phylogeny for each continuous character using the function `fitContinuous` in the R package *geiger* (Harmon et al. 2007). The models compared were the white noise (WN; non-phylogenetic model that assumes all values come from a single normal distribution with no covariance structure among species), the Brownian Motion (BM) model of neutral divergent evolution (Martins 1996), the Early Burst (EB) model of decreasing rate of evolutionary change (Harmon et al. 2010), and the Ornstein-Uhlenbeck (OU) model of stabilizing selection around a fitted

212 optimum state (Uhlenbeck and Ornstein 1930; Butler and King 2004). We then ranked the
213 models in order of increasing parametric complexity (WN,BM,EB,OU), and compared the
214 corrected Akaike Information Criterion (AICc) support scores (Sugiura 1978) to the lowest
215 (best) score, using a cutoff of 2 units to determine significantly better support. When the
216 best fitting model was not significantly better than a less complex alternative, we selected
217 the least complex model (Appendix 12). We calculated model adequacy scores using the
218 R package *arbutus* (Pennell et al. 2015) (Appendix 13). We calculated phylogenetic signal
219 in each of the measured characters using Blomberg's K (Blomberg et al. 2003) (Appendix
220 12). We reconstructed ancestral states using Maximum Likelihood (R phytools::anc.ML
221 (Revell 2012)), and stochastic character mapping (R phytools::make.simmap) for categorical
222 characters. R scripts available in Dryad.

223 In order to study the evolution of predatory specialization, we reconstructed components
224 of the diet and prey selectivity on the phylogeny using ML (R phytools::anc.ML). To identify
225 evolutionary associations of diet with tentillum and nematocyst characters, we compared the
226 performance of a neutral evolution model to that of a diet-driven directional selection model.
227 First, we collapsed the diet data into the five feeding guilds mentioned above (fish specialist,
228 small crustacean specialist, large crustacean specialist, gelatinous specialist, generalist), based
229 on which prey types they were observed consuming most frequently. Then, we reconstructed
230 the feeding guild ancestral states using the ML function ace (package ape (Paradis et al.
231 2019)), removing tips with no feeding data. The ML reconstruction was congruent with the
232 consensus stochastic character mapping (Appendix 18). Then, using the package *OUwie*
233 (Beaulieu and O'Meara 2012), we fitted an OU model with multiple optima and rates of
234 evolution matched to the reconstructed ancestral diet regimes, a single optimum OU model,
235 and a BM null model, inspired by the analyses in (Cressler et al. 2015). Finally, we compared
236 their AICc support values to select the best fitting model (Appendix 14).

237 To model the evolutionary associations between individual tentillum and nematocyst
238 characters and the ability to capture particular prey types in the diet, we ran a series of

239 phylogenetic generalized linear models (R `phylolm`::`phyloglm`) (Appendix 17). In addition,
240 we ran a series of comparative analyses to address hypotheses of diet-tentillum relationships
241 posed in the literature. To test for correlated evolution among binary characters, we used
242 Pagel's test (Pagel 1994). To characterize and evaluate the relationship between continuous
243 characters, we used phylogenetic generalized least squares regressions (PGLS) (Grafen 1989).
244 To compare the evolution of continuous characters with categorical aspects of the diet, we
245 carried out a phylogenetic logistic regression (R `nlme`::`gls` using the 'corBrownian' function
246 for the argument 'correlation').

247 To generate hypotheses about the diets of understudied siphonophores for which no feeding
248 observations have yet been reported (but for which we have tentacle morphology data), we
249 carried out linear discriminant analysis of principal components (DAPC) using the `dapc`
250 function (R `adegenet`::`dapc`) (Jombart et al. 2010). This function allowed us to incorporate
251 more predictors than individuals. We generated discriminant functions for feeding guild,
252 soft/hard bodied prey, and for the presence of copepods, fish, and shrimp (large crustaceans) in
253 the diet (Appendix 15). Some taxa have inapplicable states for certain absent characters (such
254 as the length of a nematocyst subtype that is not present in a species), which are problematic
255 for DAPC analyses. We tackled this by transforming the absent states to zeroes. This
256 approach allows us to incorporate all the data, but creates an attraction bias between small
257 character states (*e.g.* small tentilla) and absent states (*e.g.* no tentilla). Absent characters are
258 likely to be very biologically relevant to prey capture and we believe they should be accounted
259 for in a predictive approach. We limited the number of linear discriminant functions retained
260 to the number of groupings in each case. We selected the number of principal components
261 retained using the a-score optimization function (R `adegenet`::`optim.a.score`) (Jombart et
262 al. 2010) with 100 iterations, which yielded more stable results than the cross validation
263 function (R `adegenet`::`xval`). This optimization aims to find the compromise value with highest
264 discrimination power with the least overfitting. From these DAPCs we obtained the highest
265 contributing morphological characters to the discriminaton (characters in the top quartile of

the weighted sum of the linear discriminant loadings controlling for the eigenvalue of each discriminant). For each DAPC we generated hypotheses about the diets of siphonophores outside the training set (R adegenet::predict.dapc), incorporating prediction uncertainty as posterior probabilities (Appendix 15). In order to identify the sign of the relationship between the predictor characters prey type presence in the diet, we then generated generalized logistic regression models (as a type of generalized linear model, or GLM using R stats::glm) with the top contributing characters (from the corresponding DAPC) as predictors. We also carried out these GLMs on the Ivlev's selectivity indices for each prey type calculated from (Purcell 1981) (in Appendix 11).

In order to explore the correlational structure among continuous characters and among their evolutionary histories, we used principal component analysis (PCA) and phylogenetic PCA (Revell 2012). Since the character dataset contains many gaps due to missing characters and inapplicable states, we carried out these analyses on a subset of species and characters that allowed for the most complete dataset. This was done by removing the terminal filament characters (which are only shared by a small subset of species), and then removing species which had inapplicable states for the remaining characters. In addition, we obtained the correlations between the phylogenetic independent contrasts (Felsenstein 1985) using the package rphylip (Revell and Chamberlain 2014).

In order to study correlations between the rates of evolution between different characters, we fitted a set of evolutionary variance covariance matrices (Revell and Collar 2009) (R phytools::evol.vcv). When fitting all covariance terms simultaneously (Appendix 20.1-20.3), we selected the largest set of characters that would allow the analysis to run without computational singularities. This excluded many of the morphometric characters which are linearly dependent on other characters. Since the functions do not tolerate missing data, we ran the analyses in two ways: One including all taxa but transforming absent states to zeroes, and another removing the taxa with absent states. To test whether phenotypic integration changes across selective regimes determined by the reconstructed feeding guilds,

293 we carried out character-pairwise variance covariance analysis comparing alternative models
294 (R phytools::evolcv.lite), including those where correlations are the same across the whole
295 tree and models where correlations differ between selective regimes. These analyses could
296 only be carried out on the subset of taxa for which diet data is available, and only among
297 character pairs that are not computationally singular for that taxonomic subset. Finally, we
298 compared regime-specific variance covariance matrices to the general matrix and to their
299 preceding regime matrix to identify the changes in character dependence unique to each
300 regime (see Appendix 20). Gelatinous specialist correlations could only be estimated for a
301 small subset of characters present in *Apolemia*, and should be interpreted with care.

302 To test how many times extreme nematocyst morphologies evolved, we reconstructed
303 the ancestral states of $\log(\text{length}/\text{width})$ of the different cnidoband nematocyst types, and
304 identified the branches with the greatest shifts. In addition to characterizing the shifts in the
305 state values of haploneme and heteroneme elongation, we identified and located regime shifts
306 for the rate of evolution using a Bayesian Analysis of Macroevolutionary Mixtures (BAMM)
307 (Rabosky et al. 2014) (Appendix 16).

308 Results

309 *Phylogeny* – Only 5 nodes (blue dots in Figure 4) in the unconstrained inference were
310 incongruent with the (Munro et al. 2018) transcriptome tree, and these were constrained
311 during estimation of the 18S+16S tree. The topology of the constrained tree presented here
312 (Fig. 4) is congruent with the resolved nodes in (Dunn et al. 2005) and (Munro et al. 2018).

313 We retained the clade nomenclature defined in (Dunn et al. 2005) and (Munro et al.
314 2018), such as Codonophora to indicate the sister group to Cystonectae, Euphysonectae to
315 indicate the sister group to Calycophorae, Clade A and B to indicate the two main lineages
316 within Euphysonectae. In addition, we define two new clades within Codonophora (Fig. 4):
317 Eucladophora as the clade containing *Agalma elegans* and all taxa that are more closely related
318 to it than to *Apolemia lanosa*, and Tendiculophora as the clade containing *Agalma elegans* and

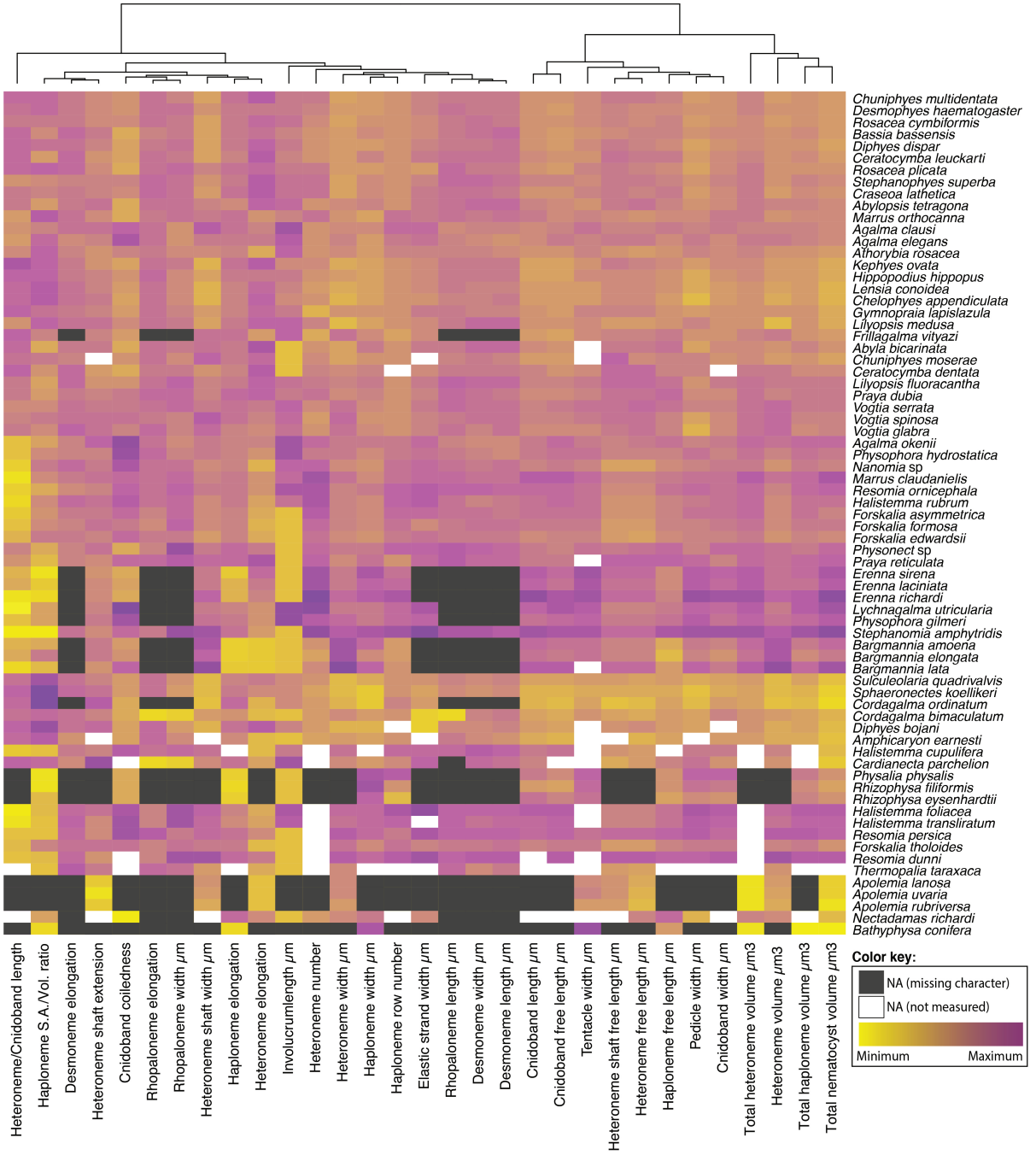


Figure 3: Heatmap summarizing the morphological diversity measured for 96 species of siphonophores clustered by similarity (raw data in Appendix 3). Missing values from absent characters presented as dark grey cells, missing values produced from technical difficulties presented as white cells. Values scaled by character.

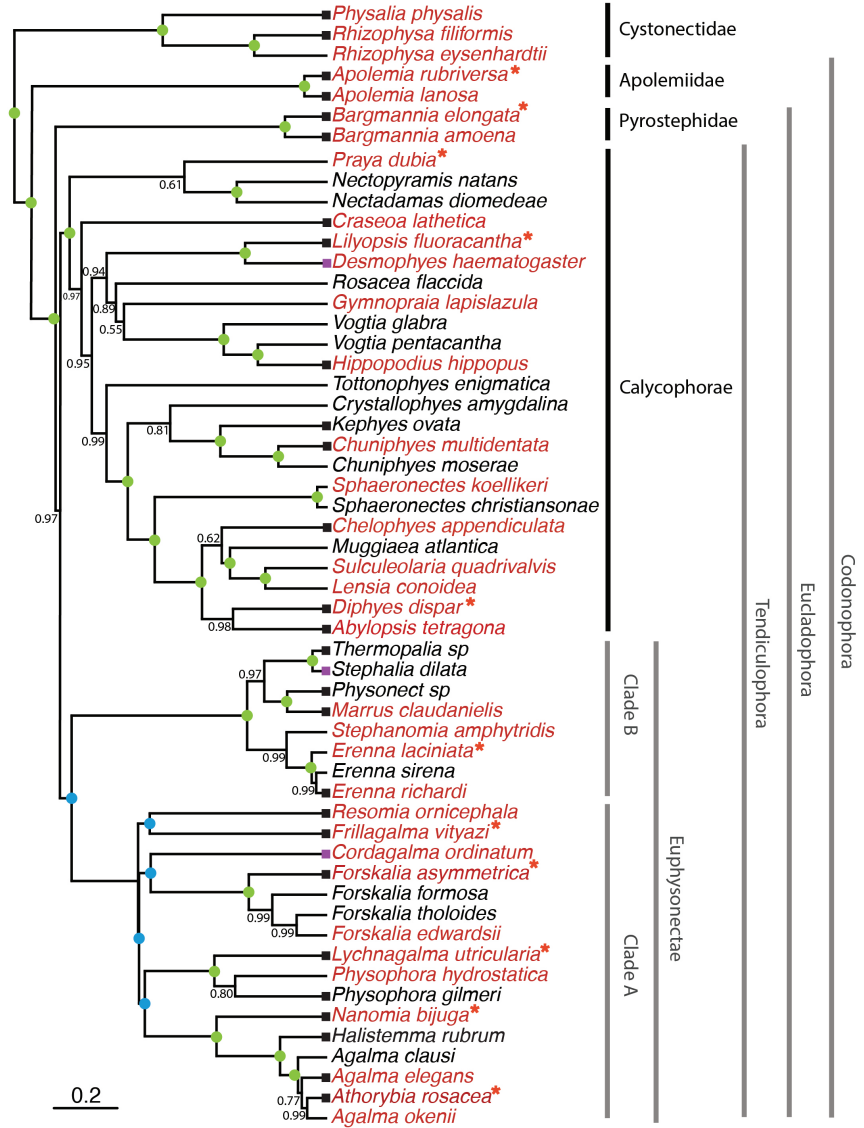


Figure 4: Bayesian time-tree built from 18S + 16S concatenated sequences. Branch lengths estimated using relaxed molecular clock. Species names in red indicate replicated representation in the morphology data. Species marked with an asterisk were recorded using high speed video. Nodes labeled with bayesian posteriors (BP). Green circles indicate BP = 1. Blue circles indicate nodes constrained to be congruent with (Munro *et al.* 2018). Tips with black squares indicate the species with transcriptomes used in (Munro *et al.* 2018). Tips with grey squares indicate genus-level correspondence to taxa included in (Munro *et al.* 2018). The main clades are labeled: in black for described taxonomic units, and in grey for operational phylogenetic designations.

319 all taxa more closely related to it than to *Bargmannia elongata*. Eucladophora is characterized
320 by bearing spatially differentiated tentilla with proximal heteronemes and a narrower terminal
321 filament region. The etymology derives from the Greek *eu+kládos+phóros* for “true branch
322 bearers”. Tendiculophora are characterized by bearing rhopalonemes and desmonemes in the
323 terminal filament, having a pair of elastic strands, and developing proximally detachable
324 cnidobands. The etymology of this clade is derived from the Latin *tendicula* for “snare or
325 noose” and the Greek *phóros* for “carriers”.

326 *Evolutionary dynamics between diet and tentillum morphology* – Reconstructions of feeding
327 guilds shows that generalism is not likely to be ancestral, and it appears to have evolved at
328 least two times independently (Fig. 5). Large crustacean specialists evolve into generalists
329 twice independently, supporting hypothesis 3. Feeding guild specializations have shifted
330 from an alternative ancestral state at least five times, supporting hypothesis 2. Copepod
331 specialization and fish specialization evolved twice, and ostracod specialization evolved at
332 least once.

333 The OUwie model comparison shows that out of 30 characters, 10 show significantly
334 stronger support for the diet-driven multi-optima multi-rate OU model (Appendix 14). These
335 characters include terminal filament nematocyst size and shape, involucrum length, elastic
336 strand width, and heteroneme number. Most of these characters are found exclusively in
337 Tendiculophora, thus this may reflect processes that could be unique to this subtree. Five
338 characters including cnidoband length, cnidoband shape, and haploneme length show maximal
339 support for a diet-driven single-optimum OU model. The remaining 15 characters support
340 BM (or OU with marginal AICc difference with BM).

341 Phylogenetic logistic regressions identified evolutionary associations between individual
342 characters and the presence of particular prey types in the diet (Fig. 5, right). Shifts toward
343 ostracod presence in diet correlated with reductions in pedicle width and total haploneme
344 volume. Shifts to copepod presence in the diet were associated with reductions in haploneme
345 width, cnidoband length and width, total haploneme and heteroneme volumes, and tentacle

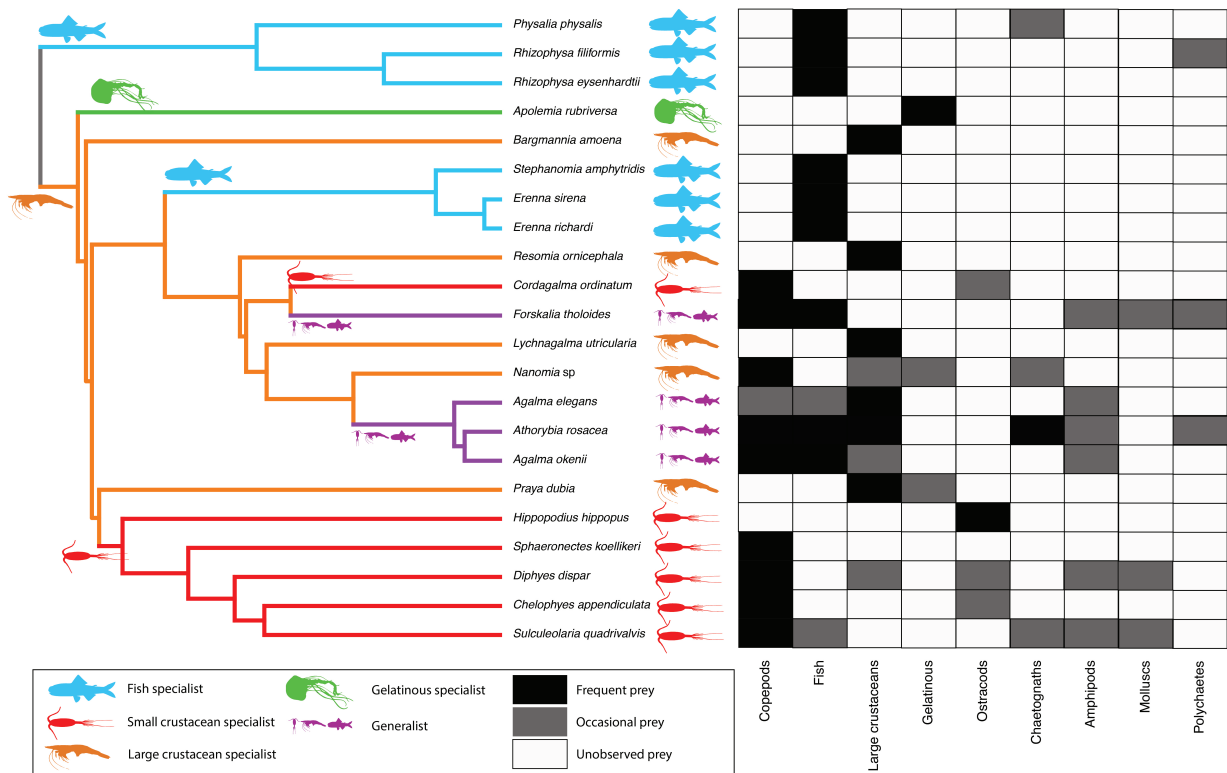


Figure 5: Left - Subset phylogeny showing the mapped feeding guild regimes that were used to inform the *OUwie* analyses. Right - Grid showing the prey items consumed from which the feeding guild categories were derived. Diet data were obtained from the literature review in Appendix 10.

346 and pedicle widths. Consistently, transitions to decapod presence in the diet correlated with
347 more coiled cnidobands (Appendix 17).

348 Phylogenetic regressions of continuous characters against prey selectivity data produced
349 additional insights. Fish selectivity is associated with increased number of heteronemes
350 per tentillum, increased roundness of nematocysts (desmonemes and haplonemes), larger
351 heteronemes, reduced heteroneme/cnidoband length ratios, smaller rhopalonemes, lower
352 haploneme SA/V ratios, and increased size of the cnidoband, elastic strand, pedicle and
353 tentacle widths. Decapod-selective diets were associated with increasing cnidoband size and
354 coiledness, haploneme row number, elastic strand width, and heteroneme number. Copepod-
355 selective diets evolved in association with smaller heteroneme and total nematocyst volumes,
356 smaller cnidobands, rounder rhopalonemes, elongated heteronemes, narrower haplonemes
357 with higher SA/V ratios, and smaller heteronemes, tentacles, pedicles and elastic strands.
358 Selectivity for ostracods was associated with reductions in size and number of heteroneme
359 nematocysts, reductions in cnidoband size, number of haploneme rows, heteroneme number,
360 and cnidoband coiledness. Heteroneme length and elongation also correlated negatively with
361 chaetognath selectivity.

362 When some of the diet-morphology associations reported in the literature (Purcell 1984;
363 Purcell and Mills 1988) were tested for correlated evolution (Table 1), we found that most
364 were consistent with an evolutionary explanation except the relationship between terminal
365 filament nematocysts (rhopalonemes and desmonemes) and crustaceans in the diet. The latter
366 is likely a product of the larger species richness of crustacean-eating species with terminal
367 filament nematocysts, rather than simultaneous evolutionary gains.

368 Table 1. Tests of correlated evolution between morphological characters and aspects of
369 the diet found correlated in the literature.

Character	Aspect of diet	Test of evolutionary association	Relationship sign	P-value	Number of taxa	Association first report
Differentiated cnidobands	Hard bodied prey	Page's test	+	0.017	19	Purcell, 1984
Heteroneme volume	Copepod prey size	pGLS	+	0.002	8	Purcell, 1984
Terminal filament nematocysts	Crustacean diet	Page's test	Non-Significant	0.200	19	Purcell & Mills, 1988
Number of nematocyst types	Soft-bodied prey	Phylogenetic logistic regression	-	0.040	22	Purcell & Mills, 1988

370

371

372 *Generating dietary hypotheses using tentillum morphology* – The discriminant analysis of
373 principal components for feeding guild (7 principal components, 4 discriminants) produced
374 100% discrimination, and the highest loading contributions were found for the characters
375 (ordered from highest to lowest): Involucrum length, heteroneme volume, heteroneme number,
376 total heteroneme volume, tentacle width, heteroneme length, total nematocyst volume, and
377 heteroneme width (Appendix 15.1). We used the predictions from this discriminant function
378 to generate hypotheses about the feeding guild of 45 species in our morphological data (Fig.
379 @figure6)). This projection predicts that two other *Apolemia* species may also be gelatinous
380 prey specialists like *Apolemia rubriversa*, and that *Erenna laciniata* may be a fish specialist
381 like *Erenna richardi*.

382 Table 2. Discriminant analysis of principal components for the presence of specific prey
383 types using the morphological data. Top quartile variable (character) contributions to the
384 linear discriminants are ordered from highest to lowest. Logistic regressions and GLMs
385 were fitted to predict prey type presence and selectivity respectively. The sign of the slope
386 of each predictor is reported, marked with an asterisk if significant (p value < 0.05), and
387 highlighted grey if it differs between prey presence in diet and prey selectivity. Pseudo- R^2
388 (%) approximates the percent variance explained by the model.

Prey type	DAPC	GLM for prey type presence (22 taxa)			Best fitting GLM for prey type selectivity (Purcell, 1981) (7 taxa)	
		Discrimination (%)	Top quartile variable contributions	Sign	Pseudo-R ² (%)	Sign
Copepods	95.4	Total nematocyst volume	-	-*		
		Tentacle width	-	+		
		Haploneme elongation	-	+		
		Haploneme surface area/volume ratio	+		67.8	-
		Haploneme row number	+	+		97.9
		Cnidoband length	-	+		
		Cnidoband width	-	-		
		Cnidoband free length	+	+		
Fish	68.1	Total haploneme volume	-	+		
		Heteroneme volume	+	-		
		Total nematocyst volume	-	+		
		Total heteroneme volume	-	-	45.8	
		Cnidoband length	-	-		96.0
		Cnidoband free length	+	+		
		Involucrum length	-	-		
		Pedicle width	+	+		
Large crustaceans	81.8	Involucrum length	+	+		
		Total heteroneme volume	-	-		
		Elastic strand width	-	+		
		Rhopaloneme length	+	+	73.2	
		Heteroneme volume	+	-		98.7
		Haploneme elongation	-	+		
		Desmoneme length	-	-		
		Tentacle width	+	+		

389

When predicting soft- and hard-bodied prey specialization, the DAPC achieved 90.9% discrimination success, only marginally confounding hard-bodied specialists with generalists (Appendix 15.4). The main characters driving this discrimination are involucrum length, heteroneme number, heteroneme volume, tentacle width, total nematocyst volume, total haploneme volume, elastic strand width, and heteroneme length. Discriminant analyses and GLM logistic regressions were also applied to specific prey type presence and selectivity (Table 2), revealing the sign of their predictive relationship to each prey type. We only selected prey types with sufficient variation in the data to carry out these analyses (copepods, fish, and large crustaceans). While the presence of fish or large crustaceans in the diet cannot be unambiguously discriminated using tentillum morphology (Appendix 15), specialization on fish or large crustacean prey can be fully disentangled (Appendix 15.1). For each prey type studied, tentillum morphology is a much better predictor of prey selectivity than of prey presence in the diet, despite prey selectivity data being available for a smaller subset of species. Interestingly, many of the morphological predictors had opposite slope signs when predicting prey selectivity *versus* predicting prey presence in the diet (Table 2).

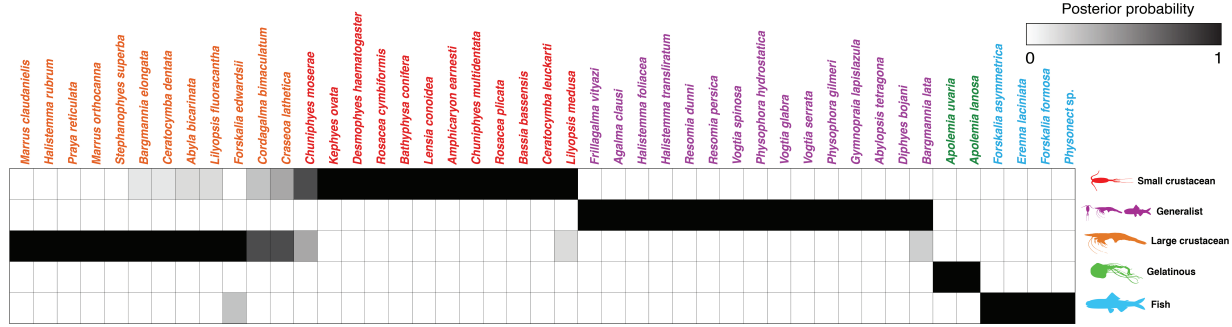


Figure 6: Hypothetical feeding guilds for siphonophore species predicted by a 6 PCA DAPC (in Appendix 15.1). Cell darkness indicates posterior probability of belonging to each guild. Training data set transformed so inapplicable states are computed as zeroes. Species ordered and colored according to their predicted feeding guild.

Evolution of tentillum and nematocyst characters – One third of the characters mea-

sured support a non-phylogenetic generative model, indicating they are not phylogenetically conserved (Appendix 12). Total nematocyst volume and cnidoband-to-heteroneme length ratio showed strongly conserved phylogenetic signals. 74% of characters present a significant phylogenetic signal, yet only total nematocyst volume, haploneme length, and heteroneme-to-cnidoband length ratio had a phylogenetic signal with $K > 1$. 67% of characters support BM models, indicating a history of neutral constant divergence. No relationship between phylogenetic signal and BM model support was found. Haploneme nematocyst length is the only character with support for an EB model of decreasing rate of evolution with time. No character had support for a single-optimum OU model (when uninformed by feeding guild regime priors).

The phylogenetic positions of the main categorical character shifts were reconstructed

using stochastic character mapping (Appendix 18), and summarized in Figure 7. Haploneme nematocysts are likely ancestrally present in siphonophore tentacles, since they are present in the tentacles of many other hydrozoans. Haplonemes first diverged into spherical isorhizas of 2 size classes in Cystonectae, and elongated anisorhizas of one size class in Codonophora. Haplonemes were likely lost in the tentacles of *Apolemia*, but spherical isorhizas are retained in other *Apolemia* tissues (Siebert et al. 2013). Similarly, while heteronemes exist in other tissues

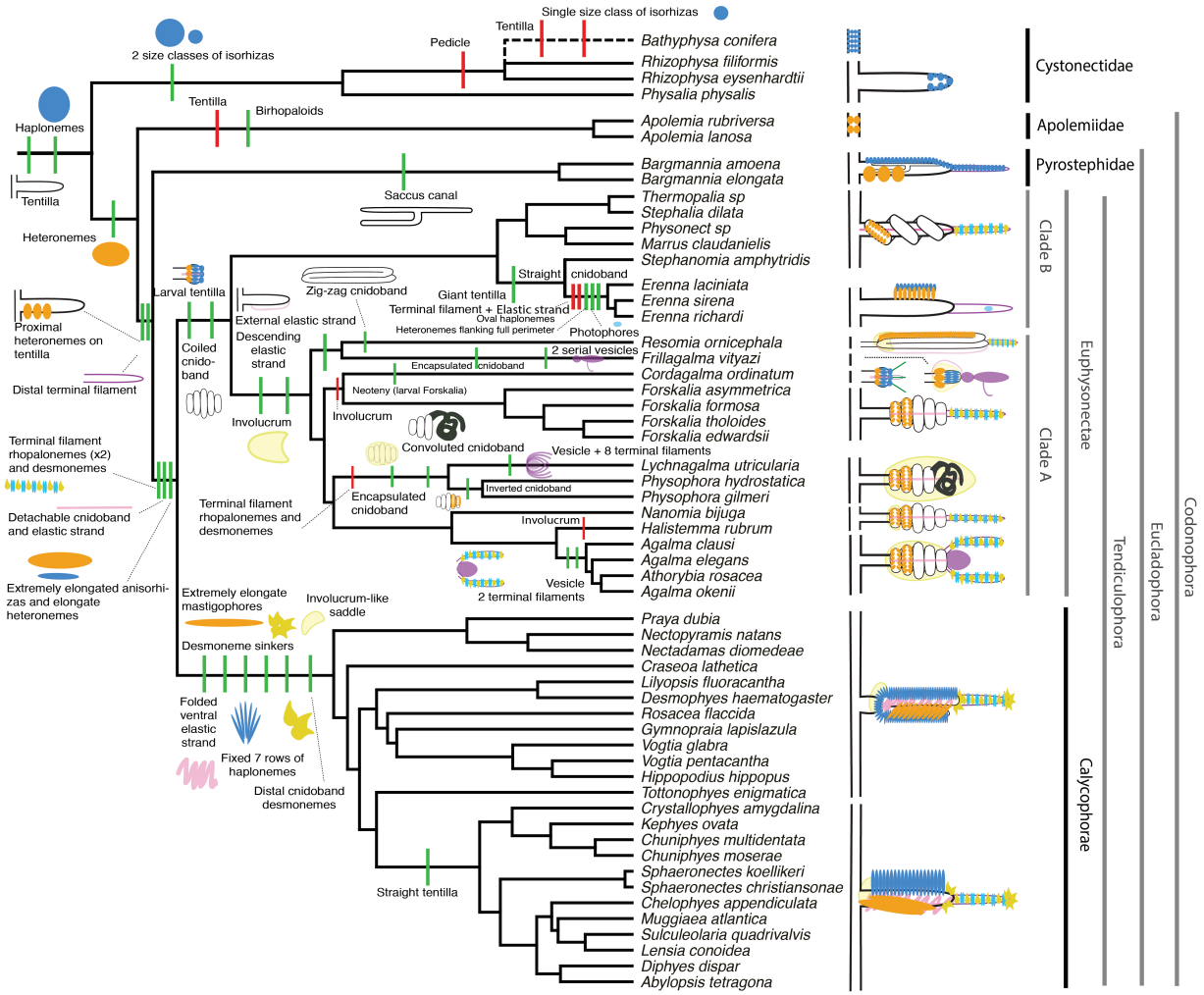


Figure 7: Siphonophore cladogram with the main categorical character gains (green) and losses (red) mapped. Some branch lengths were modified from the Bayesian chronogram to improve readability. The main visually distinguishable tentillum types are sketched next to the species that bear them, showing the location and arrangement of the main characters. In large, complex-shaped euphysonect tentilla, haplonemes were omitted for simplification. The rhizophysid *Bathypysa conifera* branch was appended manually as a polytomy (dashed line).

423 of cystonects, they appear in the tentacles of codonophorans exclusively, as birhopaloids in
424 *Apolemia*, ancestral stenoteles in eucladophoran physonects, and microbasic mastigophores in
425 calycophorans.

426 Eucladophora (the clade containing Pyrostephidae, Euphysonectae, and Calycophorae,
427 see Fig. 4) encompasses most of the extant Siphonophore species (178 of 186) other than
428 Cystonects and *Apolemia*. Innovations evolved in the stem of this group include spatially
429 segregated heteroneme and haploneme nematocysts, terminal filaments, and elastic strands
430 (Fig. 7). Pyrostephids evolved a unique bifurcation of the axial gastrovascular canal of
431 the tentillum known as the “saccus” (Totton and Bargmann 1965). The stem to the clade
432 Tendiculophora (clade containing Euphysonectae and Calycophorae, see Fig. 4) subsequently
433 acquired further novelties such as the desmoneme and rhopaloneme (acrophore subtype
434 ancestral) nematocysts on the terminal filament (Fig. 7), which bears no other nematocyst
435 type (Fig. 1). These are arranged in sets of 2 parallel rhopalonemes for each single desmoneme
436 (Skaer 1988, 1991). The involucrum is an expansion of the epidermal layer that can cover part
437 or all of the cnidoband (Fig. 2). This structure, together with differentiated larval tentilla,
438 appeared in the stem branch to Clade A physonects. Calycophorans evolved novelties such as
439 larger desmonemes at the distal end of the cnidoband, pleated pedicles with a “hood” (here
440 considered homologous to the involucrum) at the proximal end of the tentillum, anacrophore
441 rhopalonemes, and microbasic mastigophore-type heteronemes. While calycophorans have
442 diversified into most of the extant described siphonophore species (108 of 186), their tentilla
443 have not undergone any major categorical gains or losses since their most recent common
444 ancestor. Nonetheless, they have spread over a broad span of variation in nematocyst and
445 cnidoband sizes.

446 *Phenotypic integration of the tentillum* – The quantitative characters we measured from
447 tentilla and their nematocysts are highly correlated. The results indicate that the dimen-
448 sionality of tentillum morphology is low, that many traits are associated with size, but that
449 nematocyst arrangement and shape are independent of it. Of the phylogenetic correlations

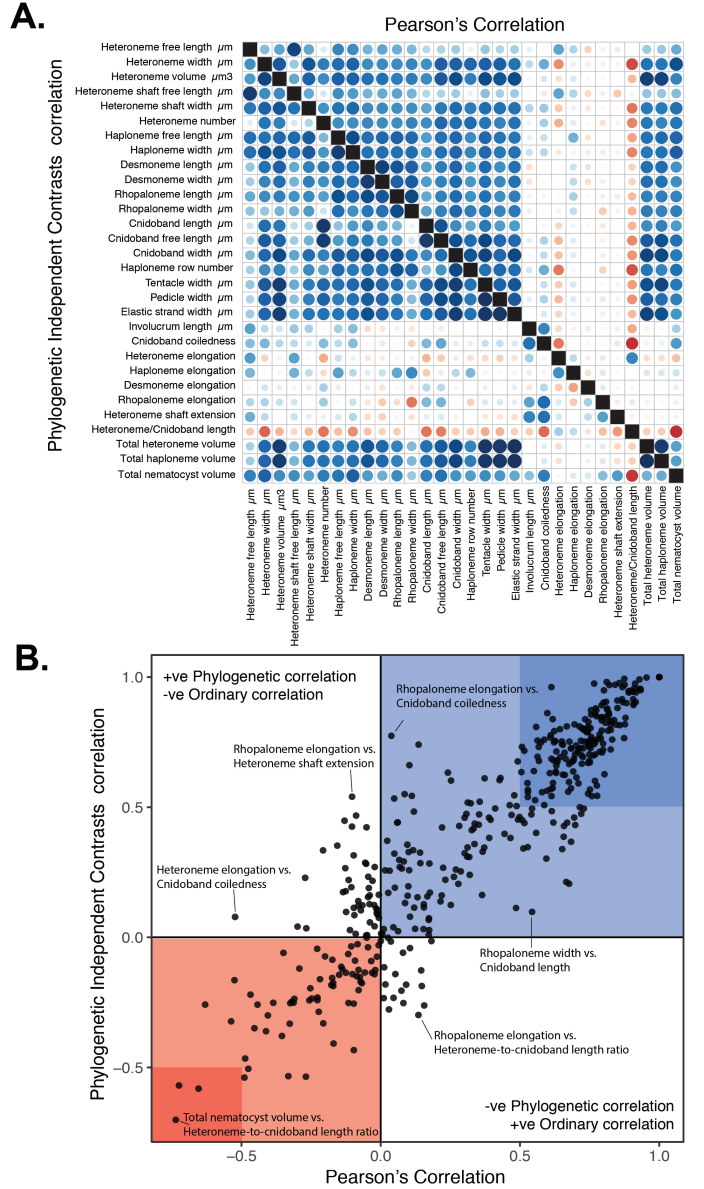


Figure 8: A. Correlogram showing strength of ordinary (upper triangle) and phylogenetic (lower triangle) correlations between characters. Both size and color of the circles indicate the strength of the correlation (R^2). B. Scatterplot of phylogenetic correlation against ordinary correlation showing a strong linear relationship ($R^2 = 0.92$, 95% confidence between 0.90 and 0.93). Light red and blue boxes indicate congruent negative and positive correlations respectively. Darker red and blue boxes indicate strong (<-0.5 or >0.5) negative and positive correlation coefficients respectively.

450 (Fig. 8a, lower triangle), 81.3% were positive and 18.7% were negative, while of the ordinary
451 correlations (Fig. 8a, upper triangle) 74.6% were positive and 25.4% were negative. Half
452 (49.9%) of phylogenetic correlations were >0.5 , while only 3.6% are <-0.5 . Similarly, of the
453 across-species correlations, 49.1% were >0.5 and only 1.5% were <-0.5 . We found that 13.9%
454 of character pairs had opposing phylogenetic and ordinary correlation coefficients. Just 4%
455 have negative phylogenetic and positive ordinary correlations (such as rhopaloneme elongation
456 \sim heteroneme-to-cnidoband length ratio and haploneme elongation, or haploneme elongation
457 \sim heteroneme number), and only 9.9% of character pairs had positive phylogenetic correlation
458 yet negative ordinary correlation (such as heteroneme elongation \sim cnidoband convolution
459 and involucrum length, or rhopaloneme elongation with cnidoband length). These disparities
460 can be caused by Simpson's paradox (Blyth 1972): the reversal of the sign of a relationship
461 when a third variable (or a phylogenetic topology (Uyeda et al. 2018)) is considered. However,
462 no character pair had correlation coefficient differences larger than 0.64 between ordinary
463 and phylogenetic correlations (heteroneme shaft extension \sim rhopaloneme elongation has a
464 Pearson's correlation of 0.10 and a phylogenetic correlation of -0.54). Rhopaloneme elongation
465 shows the most incongruencies between phylogenetic and ordinary correlations with other
466 characters.

467 The variance covariance matrices (Appendix 20.1-20.2) are congruent with the abundant
468 positive correlations observed among simple measurement characters in Fig. 8a. However,
469 this analysis reveals more clearly the diagonal blocks that constitute the evolutionary modules,
470 such as the heteroneme block, the terminal filament nematocyst block, and the cnidoband-
471 pedicle-tentacle block. These results were not very sensitive to transformation of inapplicable
472 states and taxon sampling. When we compared the rate covariance terms between characters
473 across the different feeding guild regimes (Appendix 20.4), we found that half (48%) of the
474 character pairs presented distinct correlation coefficients across different regimes, indicating
475 that the mode of phenotypic integration may also shift with trophic niche. When contrasting
476 the regime-specific rate correlation matrices to the whole-tree matrix, we were able to identify

477 the character dependencies that are unique to each predatory niche (Appendix 20.6).

478 Under the majority of SIMMAP outcomes, large crustaceans specialists are the first regime
479 to appear, and other regimes evolve in a shift from this ancestral specialization. Compared
480 to the rate correlation matrix estimated over the whole tree, large crustacean specialists
481 present strong negative correlations between haploneme elongation and heteroneme size,
482 and between rhopaloneme elongation and tentillum size, as well as with involucrum length.
483 With the appearance of generalists (*Forskalia* and the *Agalma-Athorybia* clade), terminal
484 filament nematocyst (desmonemes and rhopalonemes) sizes became negatively correlated with
485 the sizes of most characters, meaning that as some tentilla became larger, their individual
486 terminal nematocysts became smaller, observed to the extreme in *Agalma*. In addition,
487 heteroneme and rhopaloneme elongation became positively correlated with cnidoband size.
488 When large crustacean specialists switched to small crustacean prey in *Cordagalma* and
489 calycophorans, haploneme size became inversely correlated with heteroneme elongation,
490 which in turn developed a strong positive relationship with tentillum size. In other words, as
491 tentilla get smaller in this group, heteronemes get shorter and haplonemes get larger. The
492 extremes of this gradient can be seen in *Cordagalma* and *Hippopodius*. With the evolution
493 of fish prey specialization in cystonects and within Clade B, haploneme elongation became
494 negatively correlated with heteroneme elongation (signal driven by Clade B, since cystonects
495 lack tentacular heteronemes), and the surface area to volume ratio of haploneme nematocysts
496 switched from a strong negative relationship with cnidoband size (found in every other
497 regime) to a positively correlation. Gelatinous specialization, albeit appearing only once in
498 our tree, also carries a unique signature in character rate correlation shifts, with an increase
499 in the strength of the correlation between heteroneme shape and shaft width, consistent with
500 the appearance of birhopaloid nematocysts with swollen shafts that are likely effective at
501 anchoring gelatinous tissue (see reference to Narcomedusae nematocysts in (Purcell and Mills
502 1988)).

503 In the non-phylogenetic PCA morphospace using only simple characters (Fig. 9), PC1

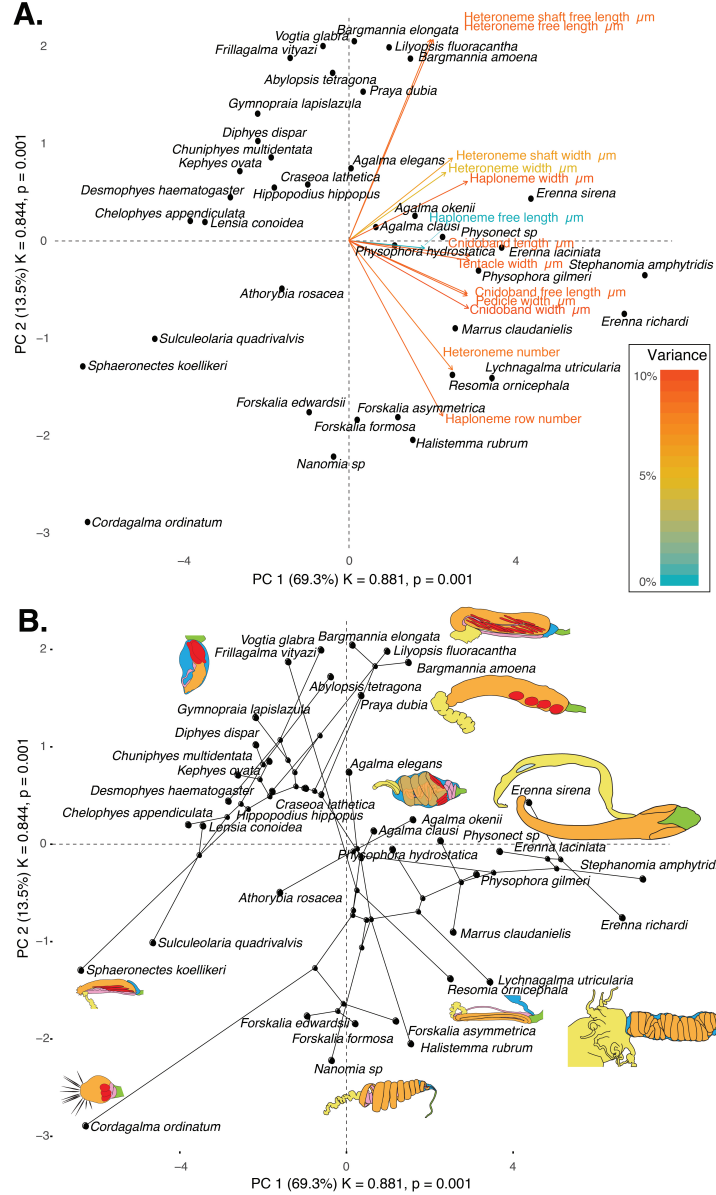


Figure 9: Phylomorphospace of the simple continuous characters principal components, excluding ratios and composite characters. A. Variance explained by each variable in the PC1-PC2 plane. Axis labels include the phylogenetic signal (K) for each component and p-value. B. Phylogenetic relationships between the species points distributed in that same space.

504 (aligned with tentillum and tentacle size) explained 69.3% of the variation in the tentillum
505 morphospace, whereas PC2 (aligned with heteroneme length, heteroneme number, and
506 haploneme arrangement) explained 13.5%. In a phylogenetic PCA, 63% of the evolutionary
507 variation in the morphospace is explained by PC1 (aligned with shifts in tentillum size), while
508 18% is explained by PC2 (aligned with shifts in heteroneme number and involucrum length).

509 *Evolution of nematocyst shape* – Haploneme nematocyst evolution has been mainly driven
510 by a single large shift towards elongation in Tendiculophora, which contains the majority of
511 described siphonophore species other than Cystonects, *Apolemia*, and Pyrostephidae. There
512 is one secondary return to more oval, less elongated haplonemes in *Erenna*, but it does not
513 reach the sphericity present in Cystonectae or Pyrostephidae (Fig. 10). Heteroneme evolution
514 presents a less discrete evolutionary history, where Tendiculophora evolved more elongate
515 heteronemes, but the difference between theirs and other siphonophores is much smaller than
516 the variation in shape within Tendiculophora, bearing no phylogenetic signal. In this clade,
517 evolution of heteroneme shape has diverged in both directions, and there is no correlation
518 with haploneme shape (Fig. 10), which has remained fairly constant (elongation between 1.5
519 and 2.5).

520 Haploneme and heteroneme shape share 21% of their variance across extant values, and
521 53% of variance in their shifts along the branches of the phylogeny. However, much of this
522 correlation is due to the contrast between Pyrostephidae and their sister group Tendiculophora
523 (Fig. 4). BAMM identified a regime shift in heteroneme shape evolution on the branches
524 leading to *Agalma* and *Athorybia*. For the rates of haploneme shape evolution, BAMM
525 identified two main independent regime shifts (Fig. 10): one in the branch leading to
526 Codonophora (anisorhizas diverging from cystonects' spherical isorhizas), and one in the
527 branch leading to Clade B physonects. Clade B includes *Erenna*, *Stephanomia*, *Marrus*, and
528 rhodaliids. Most of these taxa have rod-shaped anisorhizas, but *Erenna* has oval ones). No
529 clear regime shift patterns were identified in the evolution of desmoneme and rhopaloneme
530 shape.

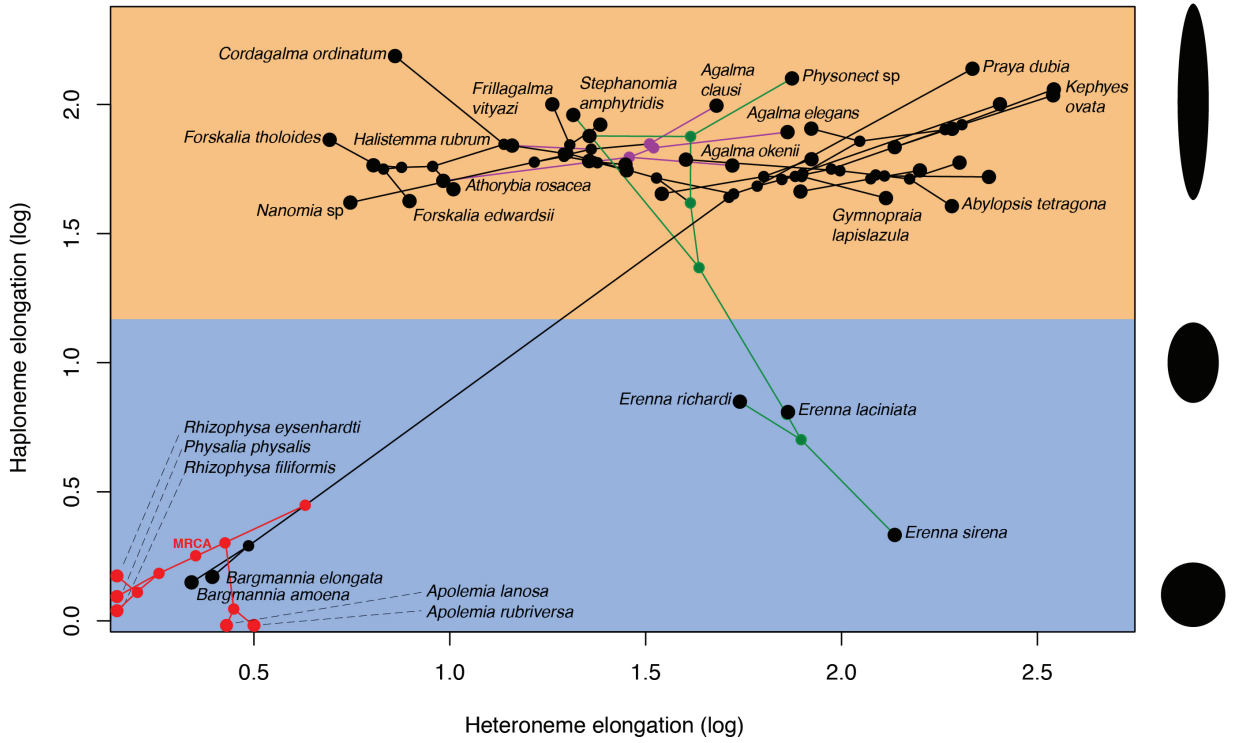


Figure 10: Phylomorphospace showing haploneme and heteroneme elongation (log scaled). Orange area delimits rod-shaped haplonemes, blue area covers oval and round shaped haplonemes. Smaller dots and lines represent phylogenetic relationships and ancestral states of internal nodes under BM. Species nodes in red were manually added to the plot. Cystonects have no tentacle heteronemes and are projected onto the haploneme axis. Apolemiids have no tentacle haplonemes and are projected onto the heteroneme axis. Colored branches and nodes correspond to BAMM regimes of accelerated haploneme shape (green) and heteroneme shape (violet) evolution.

531 *Functional morphology of tentillum and nematocyst discharge* – Tentillum and nematocyst
532 discharge high speed measurements are available in Appendix 4. While the sample sizes of
533 these measurements were insufficient to draw reliable statistical results at a phylogenetic level,
534 we did observe patterns that may be relevant to their functional morphology. For example,
535 cnidoband length is strongly correlated with discharge speed (*p* value = 0.0002). This is
536 probably the sole driver of the considerable difference between euphysonect and calycophoran
537 tentilla discharge speeds (average discharge speeds: 225.0mm/s and 41.8mm/s respectively;
538 *t*-test *p* value = 0.011), since the euphysonects have larger tentilla than the calycophorans
539 among the species recorded.

540 We also observed that calycophoran haploneme tubules fire faster than those of eu-
541 physonects (*T*-test *p* value = 0.001). Haploneme nematocysts discharge 2.8x faster than
542 heteroneme nematocysts (*T*-test *p* value = 0.0012). Finally, we observed that the stenoteles
543 of the Euphysonectae discharge a helical filament that “drills” itself through the medium it
544 penetrates as it everts.

545 Discussion

546 The core aims of this study are to examine the evolutionary history of siphonophore tentilla and
547 diet, characterize the evolutionary shifts in their trophic niches, and identify the morphological
548 characters that evolve with changes in prey type. We inquire whether the relationships between
549 form and function observed in extant taxa are due to correlated evolution or non-evolutionary
550 causes, whether the evolution of their trophic specializations supports or challenges traditional
551 ecological theory (such as the idea specialists evolve from generalists), and whether the diets
552 of siphonophores can be hypothesized by observing their tentacles. In addition, we produced
553 novel findings on tentillum morphology, siphonophore phylogeny, nematocyst character
554 evolution, and tentillum discharge dynamics.

555 *Evolution of tentillum morphology with diet* – Siphonophores are an abundant group of
556 zooplankton in oceanic ecosystems (Longhurst 1985; O’Brien 2007). While little is known

about siphonophore trophic ecology, what is known indicates that they occupy a central position in midwater food webs (Choy et al. 2017), serving as trophic intermediaries between smaller zooplankton and higher trophic level predators. Siphonophore species have been observed to feed on a variety of prey with very different sizes, traits, and behaviors. Because there is a total absence of siphonophores in the fossil record, how they became established as the ubiquitous and diversified predators in today's oceans remains an open question. Predators that use morphologically similar tools for prey capture tend to capture similar prey, thus their abundance and coexisting species diversity are inversely related due to competitive exclusion by resource limitation (Schluter 2000). However, this is not consistent with what we observe in siphonophores, which have been found to be both very abundant and locally diverse (Longhurst 1985, @mapstone2014global). We hypothesize that siphonophores have escaped this by specializing on different prey resources.

According to our reconstructions, the evolutionary history of siphonophore diets indicates that being a specialist was an ancestral aspect of their trophic niche, while trophic generalism is likely a derived condition. Several studies (reviewed in (Futuyma and Moreno 1988)) have suggested that resource specialization is an irreversible dead end due to the constraints posed by phenotypic specialization. Our reconstructions show that this is not the case for siphonophores, where the prey type on which they specialize has shifted at least 5 times, and generalism has evolved independently at least twice. Among the evolutionary hypotheses considered, we find support for both hypotheses 2 (specialist resource switching) and 3 (specialist to generalist), but no support for hypothesis 1 (generalist to specialist). The evolutionary history of tentilla shows that siphonophores are an example of trophic niche diversification via morphological innovation and evolution, which allowed transitions between specialized trophic niches. This strategy is particularly important in a deep open ocean ecosystem, which is a relatively homogeneous physical environment, where the primary niche heterogeneity available is the potential interactions between organisms (Robison 2004).

One of the most common prey items found in siphonophore diets is copepods (Fig. 5).

584 Copepod-specialized diets have evolved convergently in *Cordagalma* and some calycophorans.
585 These evolutionary transitions happened together with transitions to smaller tentilla with
586 fewer cnidoband nematocysts. Tentilla are expensive single-use structures, therefore we would
587 expect that specialization in small prey would beget reductions in the size of the prey capture
588 apparatus to the minimum required for the ecological performance. *Cordagalma*'s tentilla
589 strongly resemble the larval tentilla (only found in the first-budded feeding body of the
590 colony) of their sister genus *Forskalia* spp. This indicates that the evolution of *Cordagalma*
591 tentilla could be a case of paedomorphosis associated with predatory specialization on smaller
592 prey.

593 (Purcell 1984) showed that haplonemes have a penetrating function as isorhizas in
594 cystonects and an adhesive function as anisorrhizas in Tendiculophora. The two clades that
595 have been observed primarily feeding on fish (Cystonectae and Clade B, which includes
596 *Erenna*, *Stephanomia*, *Marrus*, and rhodaliids) present an accelerated rate of haploneme
597 shape evolution towards more compact haplonemes, significantly distinct from their closest
598 relatives. Isorhizas in cystonects are known to penetrate the skin of fish during prey capture,
599 and to deliver the toxins that aid in paralysis and digestion (Hessinger 1988). *Erenna*
600 anisorrhizas are also able to penetrate human skin and deliver a painful sting (Pugh 2001)
601 (and pers. obs.), a common feature of piscivorous cnidarians like cystonects or cubozoans.

602 (Thomason 1988) hypothesized that smaller, more spherical nematocysts, with a lower
603 surface area to volume ratio, are more efficient in osmotic-driven discharge and thus have
604 more power for skin penetration. The elongated haplonemes of crustacean-eating Tendicu-
605 lophora have never been observed penetrating their crustacean prey ((Purcell 1984) and our
606 unpublished observations), and are hypothesized to entangle the prey through adhesion of
607 the abundant spines to the exoskeletal surfaces and appendages. Entangling requires less
608 acceleration and power during discharge than penetration, as it does not rely on point pressure.
609 In fish-eating cystonects and *Erenna* species, the haplonemes are much less elongated and
610 very effective at penetration, in congruence with the osmotic discharge hypothesis.

611 When we tested the diet-morphology correlation hypotheses supported in the literature
612 from a macroevolutionary perspective (Table 1), we found that most of them were consis-
613 tent with correlated evolution. The ecomorphological association between rhopalonemes,
614 desmonemes, and crustacean eaters was not congruent with a scenario of correlated evolution.
615 This is probably due to the broader set of taxa in our analyses, including multiple species
616 without desmonemes or rhopalonemes but which effectively capture crustaceans (such as
617 *Cordagalma ordinatum*, *Lychnagalma utricularia*, and *Bargmannia amoena*).

618 While our results unambiguously show that tentillum morphology evolved with diet, the
619 conclusions we can draw from these analyses are limited by the sparse dietary data available.
620 Moreover, our analyses are not sufficient to adequately test hypotheses of adaptation, since
621 that would require evidence of changes within a population exposed to different selective
622 pressures. When interpreting these results, it is important to remember that diet is a product
623 of environmental prey availability and predator selectivity. Selectivity differences across
624 siphonophore species could be driven by other phenotypes not accounted for this study. For
625 example, tentacle-deploying behavior, positioning in the water column, sensitivity thresholds
626 for nematocyst discharge, or chemical cues to ingest a captured animal. Further observations
627 on these behaviors in the field are necessary to assess their relative importance in determining
628 dietary composition. In addition to behavior, there is much biochemistry in the prey capture
629 and digestion processes that remains unexplored. Part of the success in siphonophore prey
630 capture is likely determined by the effectivity of the toxins delivered by the nematocysts
631 on different taxa. Comparative toxin assays and venom protein evolution studies would
632 shed light on this question. Moreover, siphonophore trophic specialization may have brought
633 changes in the digestive biochemistry of gastrozooids and palpons. A comparison of the gene
634 expression levels for different enzymes in the gastrozooids of different species, together with
635 digestive enzyme sequence evolution studies, and a toxicological assay of the different venoms
636 in siphonophore nematocysts on different prey taxa, would provide a great complement to
637 our results.

638 *Generating hypotheses on siphonophore feeding ecology* – One motivation for our research
639 was to understand the links between predator capture tools and their diets so we can generate
640 hypotheses about the diets of siphonophores based on morphological characteristics. Indeed,
641 our discriminant analyses were able to distinguish between different siphonophore diets
642 based on morphological characters alone. The models produced by these analyses generated
643 testable predictions about the diets of many species for which we only have morphological
644 data of their tentacles. While the limited dataset used here is informative for generating
645 tentative hypotheses, the empirical dietary data are still scarce and insufficient to cast robust
646 predictions. This reveals the need to extensively characterize siphonophore diets and feeding
647 habits. In future work, we can test these ecological hypotheses and validate these models
648 by directly characterizing the diets of some of those siphonophore species. Predicting diet
649 using morphology is a powerful tool to reconstruct food web topologies from community
650 composition alone. In many of the ecological models found in the literature, interactions
651 among the oceanic zooplankton have been treated as a black box (Mitra 2009). The ability
652 to predict such interactions, including those of siphonophores and their prey, will enhance
653 the taxonomic resolution of nutrient-flow models constructed from plankton community
654 composition data.

655 *Phenotypic integration of siphonophore tentilla* – Many tentillum characters, such as
656 nematocysts, arose from the subfunctionalization of serial homologs (David et al. 2008). Serial
657 homologs have shared genetic elements underlying their development, and are expected to
658 have phylogenetic correlations (Wagner and Schwenk 2000). In addition, these sub-structures
659 must fit and work together in synchrony to ensnare prey successfully (functional integration).
660 Character complexes that satisfy these conditions tend to be phenotypically integrated.
661 Phenotypic integration is the set of functional and genetic correlations among the traits of an
662 organism (Pigliucci 2003). These correlations have been hypothesized to direct and constrain
663 adaptive evolution (Wagner and Schwenk 2000). The siphonophore tentillum morphospace
664 has a fairly low extant dimensionality due to an evolutionary history with many synchronous,

665 correlated changes. This is consistent with strong phenotypic integration where genetic and
666 developmental correlations are maintained by natural selection to preserve function.

667 Structural correlations within the tentillum are expected from shared regulatory networks
668 within a common developmental bud (budding tentilla in the tentacle). Similarly, correlations
669 between nematocyst subtypes are also expected given their common evolutionary and develop-
670 mental origin. None of these explanations for correlated evolution are surprising, nor require
671 natural selection. However, we also found correlations between nematocyst and tentillum
672 characters. Siphonophore tentacle nematocysts (in their cnidocytes) are not produced nor
673 matured in the developing tentillum. These cnidocytes are produced by dividing cnidoblasts
674 in the basigaster (basal swelling of the gastrozooid). Once the cnidocytes have assembled the
675 nematocyst, they migrate outward along the tentacle (Carré 1972) and position themselves
676 in the tentillum according to their type and size (Skaer 1988). Thus, the developmental pro-
677 grams that produce the observed nematocyst morphologies are spatially separated from those
678 producing the tentillum morphologies. Therefore, we hypothesize the genetic correlations and
679 phenotypic integration between tentillum and nematocyst characters are maintained through
680 natural selection on separate regulatory networks, out of the necessity to work together and
681 meet the spatial, mechanical, and functional constraints of their prey capture behavior.

682 Our evolutionary rate covariance results indicate that tentilla are not only phenotypically
683 integrated, but also show patterns of evolutionary modularity, where different sets of characters
684 appear to evolve in stronger correlations among each other than with other characters. This
685 may be indicative of the underlying genetic and developmental dependencies among closely
686 homologous nematocyst types (such as desmonemes and rhopalonemes) and structures. In
687 addition, these evolutionary modules point to hypothetical functional modules. For example,
688 the coiling degree of the cnidoband and the extent of the involucrum have correlated rates of
689 evolution, while high speed videos show that the involucrum helps direct the whiplash of the
690 uncoiling cnidoband forward (towards the prey).

691 While selection acting on character states is a widely studied phenomenon, recent studies

692 have shown that selection can also act upon the patterns of character correlations and
693 phenotypic dependencies (Young and Hallgrímsson 2005; Goswami 2006; Revell and Collar
694 2009; Monteiro and Nogueira 2010; Hallgrímsson et al. 2012; Claverie and Patek 2013;
695 Caetano and Harmon 2018). This evolution of character relationships can allow lineages
696 to explore new regions of the morphospace and facilitate the appearance of ecological
697 novelties. Our results show that the patterns of phenotypic integration in siphonophore
698 tentilla vary among clades, and appear to display different relationships across shifting feeding
699 specializations. Similarly to what has been found in the feeding morphologies of fish (Collar
700 et al. 2005; Revell and Collar 2009), siphonophore tentilla may have accommodated new diets
701 by altering the correlations between characters. For example, changes in the size and shape
702 relationships between nematocyst types gave rise to the nematocyst complements specialized
703 in ensnaring small crustaceans or fish. Finally, the evolvability of phenotypic dependencies
704 likely had a large role in the evolution of the diverse tentilla morphologies we observe today
705 across siphonophores.

706 *Evolutionary history of tentillum morphology* – This study produced the most speciose
707 siphonophore molecular phylogeny to date, while incorporating the most recent findings
708 in siphonophore deep node relationships. This phylogeny revealed for the first time that
709 the genus *Erenna* is the sister to *Stephanomia amphytridis*. *Erenna* and *Stephanomia* bear
710 the largest tentilla among all siphonophores, thus their monophyly indicates that there was
711 a single evolutionary transition to giant tentilla. Siphonophore tentilla range in size from
712 ~30 µm in some *Cordagalma* specimens to 2-4 cm in *Erenna* species, and up to 8 cm in
713 *Stephanomia amphytridis* (Pugh and Baxter 2014). Most siphonophore tentilla measure
714 between 175 and 1007 µm (1st and 3rd quartiles), with a median of 373 µm. The extreme
715 gain of tentillum size in this newly found clade may have important implications for access
716 to large prey size classes.

717 Tentillum size, as well as the majority of the characters studied, supported BM evolutionary
718 models. There are two alternative hypotheses about the generative process of BM. One

⁷¹⁹ hypothesis would suggest that these characters are not under selection, and therefore diverging
⁷²⁰ neutrally (Lande 1976). The second hypothesis suggests that they are under selection, but
⁷²¹ the adaptive landscape was rapidly shifting (Hansen and Martins 1996), without leaving
⁷²² clear patterns across the phylogeny. Some of the BM supported characters are likely to have
⁷²³ evolved under the second hypothesis, since when a diet-driven regime tree was provided,
⁷²⁴ these characters preferentially supported an OU model (Appendix 14).

⁷²⁵ Siphonophore tentilla are defined as lateral, monostichous evaginations of the tentacle
⁷²⁶ gastrovascular lumen with epidermal nematocysts (Totton and Bargmann 1965). The buttons
⁷²⁷ on *Physalia* tentacles were not traditionally regarded as tentilla, but (Bardi and Marques
⁷²⁸ 2007) and our observations (Munro et al. 2018), confirm that the buttons contain evaginations
⁷²⁹ of the gastrovascular lumen, thus satisfying all the criteria for the definition. In this light,
⁷³⁰ and given that most Cystonectae bear conspicuous tentilla, we conclude (in agreement with
⁷³¹ (Munro et al. 2018)) that tentilla are likely ancestral to all siphonophores, and secondarily
⁷³² lost in *Apolemia* and *Bathyphysa conifera*.

⁷³³ The clade Tendiculophora contains far more species than its relatives Cystonectae, Apolemi-
⁷³⁴ idae, and Pyrostephidae. An increase in clade richness and ecological diversification can be
⁷³⁵ triggered by a ‘key innovation’ (Simpson 1955). The evolutionary innovation of the Tendicu-
⁷³⁶ lophora tentilla with shooting cnidobands and modular regions may have facilitated further
⁷³⁷ dietary diversification. In addition, our work identifies an interesting example of convergent
⁷³⁸ evolution. The region of the tentillum morphospace (Fig. 9) occupied by calycophorans was
⁷³⁹ independently (and more recently) occupied by the physonect *Frillagalma vityazi*. Like caly-
⁷⁴⁰ cophorans, *Frillagalma* tentilla have small C-shaped cnidobands with a few rows of anisorhizas.
⁷⁴¹ Unlike calycophorans, they lack paired elongate microbasic mastigophores. Instead, they
⁷⁴² bear three elongated stenoteles, and their cnidobands are followed by a branched vesicle,
⁷⁴³ unique to this genus. Their tentillum morphology is very different from that of other related
⁷⁴⁴ physonects, which tend to have long, coiled, cnidobands with many paired oval stenoteles.
⁷⁴⁵ Most studies on calycophoran diets have reported their prey to be primarily composed of

⁷⁴⁶ small crustaceans, such as copepods or ostracods (Purcell 1981, 1984). The diet of *Frillagalma*
⁷⁴⁷ *vityazi* is unknown, but this morphological convergence suggests that they evolved to capture
⁷⁴⁸ similar kinds of prey. Our DAPCs predict that *Frillagalma* has a generalist niche with both
⁷⁴⁹ soft and hard bodied prey, including copepods.

⁷⁵⁰ *Evolution of nematocyst shape* – The phylogenetic placement of siphonophores among the
⁷⁵¹ Hydrozoa remains an unresolved question (Munro et al. 2018). The most recent work on
⁷⁵² this front sets them as sister group to all other Hydroidolina (Kayal et al. 2015). Therefore,
⁷⁵³ there is a great uncertainty around the ancestral plesiomorphies of the common ancestor
⁷⁵⁴ of all siphonophores. This is especially true for those characters that present extreme
⁷⁵⁵ differences between Cystonectae and Codonophora (the earliest split in the siphonophore
⁷⁵⁶ phylogeny). One such character is the shape of haploneme nematocysts. A remarkable
⁷⁵⁷ feature of siphonophore haplonemes is that they are outliers to all other Medusozoa in
⁷⁵⁸ their surface area to volume relationships, deviating significantly from sphericity (Thomason
⁷⁵⁹ 1988). This suggests a different mechanism for their discharge that could be more reliant on
⁷⁶⁰ capsule tension than on osmotic potentials (Carré and Carré 1980), and strong selection for
⁷⁶¹ efficient nematocyst packing in the cnidoband (Thomason 1988; Skaer 1988). Our results
⁷⁶² show that Codonophora underwent a shift towards elongation and Cystonectae towards
⁷⁶³ sphericity, assuming the common ancestor had an intermediate state. Since we know that
⁷⁶⁴ the haplonemes of other hydrozoan outgroups are generally spheroid, it is more parsimonious
⁷⁶⁵ to assume that cystonects retain this ancestral state. Later, we observe a return to more
⁷⁶⁶ rounded (ancestral) haplonemes in *Erenna*, concurrent with a secondary gain of a piscivorous
⁷⁶⁷ trophic niche, like that exhibited by cystonects.

⁷⁶⁸ In parallel with haploneme shape, heteroneme shape evolution also presents a single,
⁷⁶⁹ large, early transition towards elongation. While cystonects do not bear heteronemes in their
⁷⁷⁰ tentacles, *Physalia physalis* bears stenoteles in other zooids (Totton and Bargmann 1965),
⁷⁷¹ hypothetically used for defense rather than for prey capture. These stenotele heteronemes are
⁷⁷² rounded like those found in pyrostephids and apolemiids, which is consistent with the story

773 of a single transition leading to the elongated heteronemes in the stem of Tendiculophora.

774 The implications of these results to the evolution of nematocyst function are that an
775 innovation in the discharge mechanism of haplonemes may have occurred during the main shift
776 to elongation. Elongate nematocysts can be tightly packed into cnidobands. We hypothesize
777 this may be a Tendiculophora lineage-specific adaptation to packing more nematocysts into
778 a limited tentillum space, as suggested by (Skaer 1988). Tendiculophora, comprised of
779 the clades Euphysonectae and Calycophorae, includes the majority of siphonophore species.
780 Among these, are the most abundant siphonophore species, and a greater morphological and
781 ecological diversity is found. We hypothesize that this packing-efficient haploeme morphology
782 may have been a key innovation leading to the diversification of this clade. However, other
783 characters that shifted concurrently in the stem of this clade may have been responsible for
784 their extant diversity.

785 Some siphonophore clades have more nematocyst types than others in the tentacles
786 (Tendiculophora has 4 types, Cystonectae and Apolemidae have 1), or different subtypes
787 (e.g. stenoteles, mastigophores, birhopaloids). In addition to the tentacles, siphonophores
788 may bear nematocysts in other parts of the colony (gastrozooids, papons, palpacles, bracts,
789 nectophores, and gonozooids) (Totton and Bargmann 1965). In this paper we only look at
790 the presence of nematocyst types in the tentacles, therefore the gains and losses reported
791 are not necessarily morphological innovations, but developmental allocations. Nonetheless,
792 siphonophores have evolved unique nematocyst types and subtypes, not present in any other
793 cnidarian, such as the two types of rhopalonemes (acrophores and anacrophores), and the
794 haploneme homotrichous anisorrhizas (Werner 1965). Both these nematocyst types evolved in
795 the stem to Tendiculophora, and are likely morphological innovations, since they have not
796 yet been found in any other tissue of any other organism. The gain of extreme elongation in
797 the haplonemes of Tendiculophora can be interpreted as part of the character shift to a novel
798 anisorrhiza subtype.

799 *Diversity of discharge dynamics* – A fundamental corollary in functional morphology is

800 that structural morphology determines functional performance (Wainwright and Reilly 1994).
801 We expected the discharge dynamics exhibited by siphonophore tentilla should vary with their
802 morphological diversity. Our results are consistent with this expectation, and we observe,
803 for example, that cnidoband size largely correlates with cnidoband discharge speed. This
804 suggests that prey escape response speed may determine the minimum cnidoband length for
805 successful capture.

806 *Insights from tentillum morphology* – The measurements taken illustrate that the mor-
807 phological diversity of siphonophore tentilla and nematocysts is remarkable, both in their
808 range of shapes and sizes, as in the dimensions and subtypes of the nematocysts they bear.
809 Siphonophores bear the largest nematocysts among Hydrozoans. The largest nematocysts
810 in our dataset (*Bargmannia lata* by volume and *Resomia dunnii* by length), are the largest
811 of all nematocysts reported for cnidarians, and therefore possibly the largest intracellular
812 organelles among all living things.

813 In addition to the insights produced in this study, the newly collected morphological
814 data provide a unique resource for future studies, and a reference dataset for siphonophore
815 identification. Many conspicuous categorical characters in siphonophore tentilla are singularly
816 diagnostic, such as: the fluorescent lures of *Resomia ornicephala*, the bioluminescent lures
817 of *Erenna* species, the unique branched vesicle of *Frillagalma vityazi*, the buoyant medusa-
818 resembling vesicle of *Lychnagalma* with 8 pseudo-tentacles, the zig-zag morphology of *Resomia*
819 species, the inverted orientation of *Physophora* cnidobands, the button-like tentilla of *Physalia*,
820 or the acorn-shaped minute tentilla of *Cordagalma* species (Fig. 7). Some categorical
821 characters are synapomorphic diagnostic characters for large clades, such as the proximal
822 tentillum heteronemes of Eucladophora, the elastic strand, rhopalonemes, and desmonemes of
823 Tendiculophora, the larval tentilla of Euphysonectae, the two-sized isorhizas of Cystonectae,
824 the saccus canal of Pyrostephidae, or the seven rows of anisorhizas in Calycophorae. These
825 characters should be used together with the classical nectophore and bract characters to
826 identify species or at least impute phylogenetic affiliation from incomplete material.

827 **Conclusions**

828 Siphonophores have diverse predatory niches in the open ocean, ranging from mid-trophic
829 small crustacean eaters to piscivorous super-carnivores. With the evolution of diversified
830 prey type specializations comes the evolution of morphologies adapted to the challenges
831 posed by different prey. The results presented here indicate that the associations found
832 between siphonophore tentilla and their prey are a product of correlated evolution in highly
833 integrated traits. While much of the literature focuses on how predatory generalists evolve
834 into predatory specialists, in siphonophores we find predatory specialists can evolve into
835 generalists, and that specialists on one prey type have directly evolved into specialists on
836 other prey types. Our extended morphological characterization shows that the relationships
837 between form and ecology hold across a large set of taxa and characters, and can be used to
838 generate hypotheses on the feeding habits of uncharacterized species. We conclude that the
839 siphonophores were able to become abundant oceanic predators by occupying a variety of
840 trophic niches facilitated by the evolution and diversification of extraordinary prey capture
841 tools on their tentacles.

842 **Supplementary Materials**

843 Data available from the Dryad Digital Repository: <http://dx.doi.org/10.5061/dryad.NNNN>
844 Online Appendices are available in https://github.com/dunnlab/tentilla_morph/
845 Supplementary_materials/Online_Appendices

846 **Funding**

847 This work was supported by the Society of Systematic Biologists (Graduate Student Award
848 to A.D.S.); the Yale Institute of Biospheric Studies (Doctoral Pilot Grant to A.D.S.); and
849 the National Science Foundation (Waterman Award to C.W.D., and NSF-OCE 1829835 to
850 C.W.D., S.H.D.H., and C. Anela Choy). A.D.S. was supported by a Fulbright Spain Graduate

851 Studies Scholarship.

852 Acknowledgements

853 We wish to thank the crew and scientists of the R/V Western Flyer, who participated in
854 the collection of many of the specimens used in this study. We also want to thank Lynne
855 Christianson and Shannon Johnson from the Monterey Bay Aquarium Research Institute
856 for their assistance in the field as well as for sequencing some of the species included in this
857 phylogeny. In addition, we wish to thank Lourdes Rojas, Daniel Drew, and Eric Lazo-Wasem
858 for their assistance in imaging the fixed specimens and managing the collections. We thank
859 Dennis Pilarczyk for organizing the prey selectivity data, and Joaquin Nunez for reviewing
860 this manuscript. Furthermore, we thank Elizabeth D. Hetherington and C. Anela Choy
861 for collating the data on siphonophore feeding and for reviewing the manuscript. Finally,
862 we thank Philip Pugh, who confirmed many of our specimen identifications and taught us
863 valuable knowledge about siphonophores.

864 References

- 865 Andersen O.G.N. 1981. Redescription of *marrus orthocanna* (kramp, 1942)(Cnidaria,
866 siphonophora). Zoological Museum, University of Copenhagen.
- 867 Bardi J., Marques A.C. 2007. Taxonomic redescription of the portuguese man-of-war,
868 *physalia physalis* (cnidaria, hydrozoa, siphonophorae, cystonectae) from brazil. Iheringia.
869 Série Zoologia. 97:425–433.
- 870 Beaulieu J., O'Meara B. 2012. OUwie: Analysis of evolutionary rates in an ou framework.
871 R package version 1.17..
- 872 Biggs D.C. 1977. Field studies of fishing, feeding, and digestion in siphonophores. Marine
873 & Freshwater Behaviour & Phy. 4:261–274.
- 874 Blomberg S.P., Garland T., Ives A.R. 2003. Testing for phylogenetic signal in comparative
875 data: Behavioral traits are more labile. Evolution. 57:717–745.

- 876 Blyth C.R. 1972. On simpson's paradox and the sure-thing principle. Journal of the
877 American Statistical Association. 67:364–366.
- 878 Butler M.A., King A.A. 2004. Phylogenetic comparative analysis: A modeling approach
879 for adaptive evolution. The American Naturalist. 164:683–695.
- 880 Caetano D.S., Harmon L.J. 2018. Estimating correlated rates of trait evolution with
881 uncertainty. Systematic biology. 68:412–429.
- 882 Carré D. 1972. Study on development of cnidocysts in gastrozooids of muggiaeae kochi
883 (will, 1844) (siphonophora, calycophora). Comptes Rendus Hebdomadaires des Seances de
884 l'Academie des Sciences Serie D. 275:1263.
- 885 Carré D., Carré C. 1980. On triggering and control of cnidocyst discharge. Marine &
886 Freshwater Behaviour & Phy. 7:109–117.
- 887 Choy C.A., Haddock S.H., Robison B.H. 2017. Deep pelagic food web structure as revealed
888 by in situ feeding observations. Proceedings of the Royal Society B: Biological Sciences.
889 284:20172116.
- 890 Claverie T., Patek S. 2013. Modularity and rates of evolutionary change in a power-
891 amplified prey capture system. Evolution. 67:3191–3207.
- 892 Collar D.C., Near T.J., Wainwright P.C. 2005. Comparative analysis of morphological
893 diversity: Does disparity accumulate at the same rate in two lineages of centrarchid fishes?
894 Evolution. 59:1783–1794.
- 895 Collins T.J. 2007. ImageJ for microscopy. Biotechniques. 43:S25–S30.
- 896 Costello J.H., Colin S.P., Gemmell B.J., Dabiri J.O., Sutherland K.R. 2015. Multi-jet
897 propulsion organized by clonal development in a colonial siphonophore. Nature communica-
898 tions. 6:8158.
- 899 Cressler C.E., Butler M.A., King A.A. 2015. Detecting adaptive evolution in phylogenetic
900 comparative analysis using the ornstein–uhlenbeck model. Systematic biology. 64:953–968.
- 901 David C.N., Özbek S., Adamczyk P., Meier S., Pauly B., Chapman J., Hwang J.S.,
902 Gojobori T., Holstein T.W. 2008. Evolution of complex structures: Minicollagens shape the

- 903 cnidarian nematocyst. Trends in genetics. 24:431–438.
- 904 Dunn C.W., Pugh P.R., Haddock S.H. 2005. Molecular phylogenetics of the siphonophora
905 (cnidaria), with implications for the evolution of functional specialization. Systematic biology.
906 54:916–935.
- 907 Felsenstein J. 1985. Phylogenies and the comparative method. The American Naturalist.
908 125:1–15.
- 909 Futuyma D.J., Moreno G. 1988. The evolution of ecological specialization. Annual review
910 of Ecology and Systematics. 19:207–233.
- 911 Goswami A. 2006. Morphological integration in the carnivoran skull. Evolution. 60:169–
912 183.
- 913 Grafen A. 1989. The phylogenetic regression. Philosophical Transactions of the Royal
914 Society of London. B, Biological Sciences. 326:119–157.
- 915 Haddock S.H., Dunn C.W. 2015. Fluorescent proteins function as a prey attractant:
916 Experimental evidence from the hydromedusa olindias formosus and other marine organisms.
917 Biology open. 4:1094–1104.
- 918 Haddock S.H., Dunn C.W., Pugh P.R., Schnitzler C.E. 2005. Bioluminescent and red-
919 fluorescent lures in a deep-sea siphonophore. Science. 309:263–263.
- 920 Haddock S.H., Heine J.N. 2005. Scientific blue-water diving. California Sea Grant College
921 Program.
- 922 Hallgrímsdóttir B., Jamniczky H.A., Young N.M., Rolian C., SCHMIDT-OTT U., Marcucio
923 R.S. 2012. The generation of variation and the developmental basis for evolutionary novelty.
924 Journal of Experimental Zoology Part B: Molecular and Developmental Evolution. 318:501–
925 517.
- 926 Hansen T.F., Martins E.P. 1996. Translating between microevolutionary process and
927 macroevolutionary patterns: The correlation structure of interspecific data. Evolution.
928 50:1404–1417.
- 929 Hardin G. 1960. The competitive exclusion principle. science. 131:1292–1297.

- 930 Harmon L.J., Losos J.B., Jonathan Davies T., Gillespie R.G., Gittleman J.L., Bryan
931 Jennings W., Kozak K.H., McPeek M.A., Moreno-Roark F., Near T.J., others. 2010. Early
932 bursts of body size and shape evolution are rare in comparative data. *Evolution: International*
933 *Journal of Organic Evolution.* 64:2385–2396.
- 934 Harmon L.J., Weir J.T., Brock C.D., Glor R.E., Challenger W. 2007. GEIGER: Investi-
935 gating evolutionary radiations. *Bioinformatics.* 24:129–131.
- 936 Hessinger D.A. 1988. Nematocyst venoms and toxins. *The biology of nematocysts.*
937 Elsevier. p. 333–368.
- 938 Hissmann K. 2005. In situ observations on benthic siphonophores (physonectae: Rhodali-
939 idae) and descriptions of three new species from indonesia and south africa. *Systematics and*
940 *Biodiversity.* 2:223–249.
- 941 Hoberg E.P., Brooks D.R. 2008. A macroevolutionary mosaic: Episodic host-switching,
942 geographical colonization and diversification in complex host–parasite systems. *Journal of*
943 *Biogeography.* 35:1533–1550.
- 944 Höhna S., Landis M.J., Heath T.A., Boussau B., Lartillot N., Moore B.R., Huelsenbeck
945 J.P., Ronquist F. 2016. RevBayes: Bayesian phylogenetic inference using graphical models
946 and an interactive model-specification language. *Systematic Biology.* 65:726–736.
- 947 Hutchinson G.E. 1961. The paradox of the plankton. *The American Naturalist.* 95:137–
948 145.
- 949 Jacobs J. 1974. Quantitative measurement of food selection. *Oecologia.* 14:413–417.
- 950 Johnson K.P., Malenke J.R., Clayton D.H. 2009. Competition promotes the evolution of
951 host generalists in obligate parasites. *Proceedings of the Royal Society B: Biological Sciences.*
952 276:3921–3926.
- 953 Jombart T., Devillard S., Balloux F. 2010. Discriminant analysis of principal components:
954 A new method for the analysis of genetically structured populations. *BMC genetics.* 11:94.
- 955 Kalyaanamoorthy S., Minh B.Q., Wong T.K., Haeseler A. von, Jermiin L.S. 2017. Mod-
956 elFinder: Fast model selection for accurate phylogenetic estimates. *Nature methods.* 14:587.

- 957 Katoh K., Misawa K., Kuma K.-i., Miyata T. 2002. MAFFT: A novel method for
958 rapid multiple sequence alignment based on fast fourier transform. Nucleic acids research.
959 30:3059–3066.
- 960 Kayal E., Bentlage B., Cartwright P., Yanagihara A.A., Lindsay D.J., Hopcroft R.R.,
961 Collins A.G. 2015. Phylogenetic analysis of higher-level relationships within hydroïdolina
962 (cnidaria: Hydrozoa) using mitochondrial genome data and insight into their mitochondrial
963 transcription. PeerJ. 3:e1403.
- 964 Lande R. 1976. Natural selection and random genetic drift in phenotypic evolution.
965 Evolution. 30:314–334.
- 966 Longhurst A.R. 1985. The structure and evolution of plankton communities. Progress in
967 Oceanography. 15:1–35.
- 968 Mackie G.O., Pugh P.R., Purcell J.E. 1987. Siphonophore Biology. Advances in Marine
969 Biology. 24:97–262.
- 970 Mapstone G.M. 2014. Global diversity and review of siphonophorae (cnidaria: Hydrozoa).
971 PLoS One. 9:e87737.
- 972 Martins E.P. 1996. Phylogenies, spatial autoregression, and the comparative method: A
973 computer simulation test. Evolution. 50:1750–1765.
- 974 Mitra A. 2009. Are closure terms appropriate or necessary descriptors of zooplankton loss
975 in nutrient–phytoplankton–zooplankton type models? Ecological Modelling. 220:611–620.
- 976 Monteiro L.R., Nogueira M.R. 2010. Adaptive radiations, ecological specialization, and
977 the evolutionary integration of complex morphological structures. Evolution: International
978 Journal of Organic Evolution. 64:724–744.
- 979 Munro C., Siebert S., Zapata F., Howison M., Serrano A.D., Church S.H., Goetz F.E.,
980 Pugh P.R., Haddock S.H., Dunn C.W. 2018. Improved phylogenetic resolution within
981 siphonophora (cnidaria) with implications for trait evolution. Molecular Phylogenetics and
982 Evolution.
- 983 Nguyen L.-T., Schmidt H.A., Haeseler A. von, Minh B.Q. 2014. IQ-tree: A fast and

- 984 effective stochastic algorithm for estimating maximum-likelihood phylogenies. Molecular
985 biology and evolution. 32:268–274.
- 986 O'Brien T.D. 2007. COPEPOD, a global plankton database: A review of the 2007
987 database contents and new quality control methodology..
- 988 Pagel M. 1994. Detecting correlated evolution on phylogenies: A general method for the
989 comparative analysis of discrete characters. Proceedings of the Royal Society of London.
990 Series B: Biological Sciences. 255:37–45.
- 991 Paradis E., Blomberg S., Bolker B., Brown J., Claude J., Cuong H.S., Desper R. 2019.
992 Package “ape”. Analyses of phylogenetics and evolution, version.:2–4.
- 993 Pennell M.W., FitzJohn R.G., Cornwell W.K., Harmon L.J. 2015. Model adequacy and
994 the macroevolution of angiosperm functional traits. The American Naturalist. 186:E33–E50.
- 995 Pigliucci M. 2003. Phenotypic integration: Studying the ecology and evolution of complex
996 phenotypes. Ecology Letters. 6:265–272.
- 997 Pugh P. 2001. A review of the genus *erenna bedot*, 1904 (siphonophora, physonectae).
998 BULLETIN-NATURAL HISTORY MUSEUM ZOOLOGY SERIES. 67:169–182.
- 999 Pugh P., Baxter E. 2014. A review of the physonect siphonophore genera *halistemma*
1000 (family agalmatidae) and *stephanomia* (family stephanomiidae). Zootaxa. 3897:1–111.
- 1001 Pugh P., Youngbluth M. 1988. Two new species of prayine siphonophore (calycophorae,
1002 prayidae) collected by the submersibles johnson-sea-link i and ii. Journal of Plankton Research.
1003 10:637–657.
- 1004 Purcell J. 1981. Dietary composition and diel feeding patterns of epipelagic siphonophores.
1005 Marine Biology. 65:83–90.
- 1006 Purcell J.E. 1980. Influence of siphonophore behavior upon their natural diets: Evidence
1007 for aggressive mimicry. Science. 209:1045–1047.
- 1008 Purcell J.E. 1984. The functions of nematocysts in prey capture by epipelagic
1009 siphonophores (coelenterata, hydrozoa). The Biological Bulletin. 166:310–327.
- 1010 Purcell J., Mills C. 1988. The correlation of nematocyst types to diets in pelagic hydrozoa.

- 1011 In “the biology of nematocysts”.(Eds da hessinger and hm lenhoff.) pp. 463–485..
- 1012 Rabosky D.L., Grundler M., Anderson C., Title P., Shi J.J., Brown J.W., Huang H.,
- 1013 Larson J.G. 2014. BAMM tools: An r package for the analysis of evolutionary dynamics on
- 1014 phylogenetic trees. *Methods in Ecology and Evolution.* 5:701–707.
- 1015 Revell L.J. 2012. Phytools: An r package for phylogenetic comparative biology (and other
- 1016 things). *Methods in Ecology and Evolution.* 3:217–223.
- 1017 Revell L.J., Chamberlain S.A. 2014. Rphylip: An r interface for phylip. *Methods in*
- 1018 *Ecology and Evolution.* 5:976–981.
- 1019 Revell L.J., Collar D.C. 2009. Phylogenetic analysis of the evolutionary correlation using
- 1020 likelihood. *Evolution: International Journal of Organic Evolution.* 63:1090–1100.
- 1021 Robison B.H. 2004. Deep pelagic biology. *Journal of experimental marine biology and*
- 1022 *ecology.* 300:253–272.
- 1023 Schindelin J., Arganda-Carreras I., Frise E., Kaynig V., Longair M., Pietzsch T., Preibisch
- 1024 S., Rueden C., Saalfeld S., Schmid B., others. 2012. Fiji: An open-source platform for
- 1025 biological-image analysis. *Nature methods.* 9:676.
- 1026 Schluter D. 2000. Ecological character displacement in adaptive radiation. *the american*
- 1027 *naturalist.* 156:S4–S16.
- 1028 Schmitz O. 2017. Predator and prey functional traits: Understanding the adaptive
- 1029 machinery driving predator–prey interactions. *F1000Research.* 6.
- 1030 Shapiro S.S., Wilk M.B. 1965. An analysis of variance test for normality (complete
- 1031 samples). *Biometrika.* 52:591–611.
- 1032 Siebert S., Pugh P.R., Haddock S.H., Dunn C.W. 2013. Re-evaluation of characters in
- 1033 apolemiidae (siphonophora), with description of two new species from monterey bay, california.
- 1034 *Zootaxa.* 3702:201–232.
- 1035 Simpson G.G. 1944. *Tempo and mode in evolution.* Columbia University Press.
- 1036 Simpson G.G. 1955. *Major features of evolution.* Columbia University Press: New York.
- 1037 Skaer R. 1988. *The formation of cnidocyte patterns in siphonophores.* Academic Press

- 1038 New York.
- 1039 Skaer R. 1991. Remodelling during the development of nematocysts in a siphonophore.
- 1040 Hydrobiologia. 216:685–689.
- 1041 Stireman-III J.O. 2005. The evolution of generalization? Parasitoid flies and the perils of
- 1042 inferring host range evolution from phylogenies. Journal of evolutionary biology. 18:325–336.
- 1043 Sugiura N. 1978. Further analysts of the data by akaike's information criterion and the
- 1044 finite corrections: Further analysts of the data by akaike's. Communications in Statistics-
- 1045 Theory and Methods. 7:13–26.
- 1046 Team R.C. 2017. R: A language and environment for statistical computing. Vienna,
- 1047 austria: R foundation for statistical computing; 2017..
- 1048 Thomason J. 1988. The allometry of nematocysts. The biology of nematocysts. Elsevier.
- 1049 p. 575–588.
- 1050 Totton A.K., Bargmann H.E. 1965. A synopsis of the siphonophora. British Museum
- 1051 (Natural History).
- 1052 Uhlenbeck G.E., Ornstein L.S. 1930. On the theory of the brownian motion. Physical
- 1053 review. 36:823.
- 1054 Uyeda J.C., Zenil-Ferguson R., Pennell M.W. 2018. Rethinking phylogenetic comparative
- 1055 methods. Systematic Biology. 67:1091–1109.
- 1056 Wagner G.P., Schwenk K. 2000. Evolutionarily stable configurations: Functional in-
- 1057 tegration and the evolution of phenotypic stability. Evolutionary biology. Springer. p.
- 1058 155–217.
- 1059 Wainwright P.C., Reilly S.M. 1994. Ecological morphology: Integrative organismal biology.
- 1060 University of Chicago Press.
- 1061 Werner B. 1965. Die nesselkapseln der cnidaria, mit besonderer berücksichtigung der
- 1062 hydriida. Helgoländer wissenschaftliche Meeresuntersuchungen. 12:1.
- 1063 Young N.M., Hallgrímsson B. 2005. Serial homology and the evolution of mammalian
- 1064 limb covariation structure. Evolution. 59:2691–2704.